

Estimating forage mass in Brazilian pasture-based livestock production systems through satellite and climate data integration

Gustavo Bayma^{a,*}, Sandra Furlan Nogueira^a, Marcos Adami^b, Edson Eyji Sano^c, Daniel Coaguila Nuñez^d, Patrícia Menezes Santos^e, José Ricardo Macedo Pezzopane^e, Célia Regina Grego^f, Antônio Heriberto de Castro Teixeira^g, Sergii Skakun^h

^a Embrapa Meio Ambiente, 13820-000 Jaguariúna, Brazil

^b Instituto Nacional de Pesquisas Espaciais, 12227-010 São José dos Campos, Brazil

^c Embrapa Cerrados, 73310-970 Brasília, Brazil

^d Instituto Federal de Educação, Ciência e Tecnologia Goiano/Centro de Excelência em Agricultura Exponencial (CEAGRE), 75905-360 Rio Verde, Brazil

^e Embrapa Pecuária Sudeste, 13560-970 São Carlos, Brazil

^f Embrapa Agricultura Digital, 13083-886 Campinas, Brazil

^g Universidade Federal de Sergipe, 49100-000 São Cristóvão, Brazil

^h University of Maryland, College Park 20742, USA

ARTICLE INFO

Keywords:

Pasture productivity
Digital agriculture
Environmental sustainability
Food security

ABSTRACT

Grasslands are vital for global food security, making reliable monitoring of forage mass (FM) essential for sustainable pasture management. The availability and quality of FM are key factors in determining the profitability of pasture-based farms. This study presents a replicable methodology for estimating FM using multi-sensor satellite data and an agrometeorological modeling framework. Conducted at the Brazilian Agricultural Research Corporation Southeast Livestock Center (Embrapa Pecuária Sudeste) in São Carlos, Brazil, the research integrates NASA's Harmonized Landsat and Sentinel-2 (HLS) imagery with climate data processed through the Simple Algorithm for Evapotranspiration Retrieving (SAFER) and Monteith's Light Use Efficiency (LUE) models. The SAFER model explained over 67 % of FM variability in three pasture-based livestock systems. A key factor in achieving accurate FM estimates was the differentiation between field green matter (GM) and total dry matter, as GM represents the most nutritious and consumable forage component. The model performed best in extensive systems, where minimal management intervention resulted in stable forage conditions. In integrated crop-livestock systems, the accuracy remained high, though fertilization and crop residue decomposition influenced FM estimates. In intensive systems, model performance was slightly lower due to higher management variability. This study contributes to the development of automated, scalable FM assessment methods, enabling systematic pasture monitoring and data-driven grazing management. The SAFER model allowed simultaneous processing of satellite imagery and climate data, increasing the accuracy of FM estimations. Future research should explore the use of higher-resolution imagery (e.g., CBERS-4A, PlanetScope) to better capture within-field variability and consider increasing the frequency of field sampling frequency (from 32 days to 15 or even 7 days) to further improve FM estimation accuracy, particularly in intensive systems.

1. Introduction

Grasslands play a vital role in global food security as they provide essential feed for ruminants raised for meat and milk production (Piipponen et al., 2022; UNCCD, 2024). In addition to forage, they

provide a range of ecosystem services, such as water infiltration, wildlife habitat, and carbon sequestration (Place, 2024). Although grasslands cover more than 70 % of the global agricultural area (FAO, 2023), they have received less attention than croplands in terms of improving productivity, resilience, and climate change adaptation (Wang et al., 2022).

* Correspondent author.

E-mail addresses: gustavo.bayma@embrapa.br (G. Bayma), sandra.nogueira@embrapa.br (S.F. Nogueira), marcos.adami@inpe.br (M. Adami), edson.sano@embrapa.br (E.E. Sano), d.coaguila.nunez@gmail.com (D.C. Nuñez), patricia.santos@embrapa.br (P.M. Santos), jose.pezzopane@embrapa.br (J.R.M. Pezzopane), celia.grego@embrapa.br (C.R. Grego), heriberto@academico.ufs.br (A.H. de Castro Teixeira), skakun@umd.edu (S. Skakun).

<https://doi.org/10.1016/j.compag.2025.110496>

Received 28 September 2024; Received in revised form 28 April 2025; Accepted 1 May 2025

0168-1699/© 2025 The Author(s). Published by Elsevier B.V. This is an open access article under the CC BY license (<http://creativecommons.org/licenses/by/4.0/>).

Brazil holds a prominent position in global livestock production, ranking as the world's second largest producer of beef, with a total production of 11.2 million tons, surpassed only by the United States with 12.3 million tons (FAO, 2023). Brazil is also the fourth largest milk producer in the world, with an output of 36 million tons. These substantial production highlights the scale and productivity of Brazil's livestock sector, contributing significantly to the global food security agenda (Castro et al., 2022; Fraundorfer, 2022).

The Brazilian Agricultural Census (IBGE, 2017) reported a significant increase in cultivated pasturelands in Brazil, growing from 74 million hectares in 1985 to 112 million hectares in 2017. An automated mapping procedure based on Landsat time series analysis, conducted by the MapBiomass Project (Souza et al., 2020), showed a comparable increase, rising from 103 million hectares to 163 million hectares over the same period.

The Brazilian livestock sector has been struggling with pasture degradation, which reduces carrying capacity due to soil erosion, nitrogen leaching, and weed invasion, among others (Dias-Filho, 2017). Currently, most of Brazilian pasturelands is experiencing some level of degradation, with 32 % classified as moderately degraded and 27 % as severely degraded (Santos et al., 2022). Improvements can be achieved through practices such as pasture rotation, optimizing cost, and investment planning, minimizing input waste and reducing unnecessary operations (Feltran-Barbieri and Feres, 2021).

The advent of new technologies has fostered the development of innovative practices in livestock production, mainly the integrated production systems, which offer potentially higher productivity and sustainability, as well as improved climate change resilience compared to specialized, intensive agricultural systems. By combining crop, livestock, and forestry management on the same land and employing techniques such as crop rotation, intercropping, and successional systems, integrated systems can enhance both crop yield and livestock productivity (Reis et al., 2020; Sekaran et al., 2021; Aquilani et al., 2022).

In 2020, integrated livestock production systems in Brazil encompassed 17.4 million hectares. Projections indicate a potential expansion of 22 – 29 million hectares by 2030 (Polidoro et al., 2021). The adoption of new technologies by farmers has led to significant improvements in productivity, animal stocking rates, livestock weight gain, and overall sustainability of farming systems (Herrero et al., 2020). These technologies have also enhanced soil fertility and microbiological activity (Capristo et al., 2021), and reduced greenhouse gas emissions (Carvalho et al., 2022).

Monitoring pasture production is critical for sustainable pasture management (Phukubye et al., 2022). Accurate and timely assessments of pasture production are also critical for guiding farmers in implementing appropriate grazing management practices. Without proper grazing management, land degradation can occur, resulting in reduced forage quality, higher disease incidence, increased livestock mortality, and a significant decline in productivity. These consequences have significant socioeconomic impacts, including lower household incomes, higher poverty, and increased food insecurity (Slayi et al., 2024).

Traditionally, field data, primarily collected from farmer reports, have been used to manage forage biomass (Chen et al., 2021). However, pasture production monitoring based on field measurements is time-consuming and geographically constrained, mostly providing accurate assessments only for small areas, lacking representativeness for larger regions (Legg and Bradley, 2019).

Remote sensing allows an effective method for monitoring pasture production of large areas with relatively high frequency. Remote sensing-based methods for assessing pasture production include vegetation indices, e.g., the Normalized Difference Vegetation Index (NDVI), to estimate biophysical parameters of grasslands, such as biomass or productivity; and factor analysis, where regional and temporal patterns and trends of pasture production are analyzed, considering the effects of climate variations (Reinermann et al., 2020).

The development of advanced remote sensing satellite systems with improved spatial and temporal resolutions (Zhang et al., 2022) presents good potential for monitoring pasture production (Gargiulo et al., 2020). These technological advancements can contribute to the development of adapted management and conservation plans for pasturelands in the context of climate change (Cheng et al., 2023). Thus, automated, large-scale monitoring systems are essential for enabling continuous observation of pasturelands (Reinermann et al., 2020).

The amount of available forage mass (FM) is crucial in determining the appropriate stocking rate for livestock (Almeida et al., 2023), as it influences both the stocking rate and grazing intensity, thereby optimizing the gain per unit of land area. The nutritional quality of the forage determines the maximum possible gain per animal. Both the quantity and quality of forage are directly related to animal performance (Rouquette Jr., 2016). Proper management of forage quantity and its nutritional value prevents overgrazing, which can cause serious problems in rangeland ecosystems and threaten human livelihoods worldwide (Varga et al., 2021). Optimizing the use of forages as a high-quality, cost-effective feed source is key to achieving profitability in pasture-based farming systems (Beukes et al., 2019).

Reliable FM estimation is essential for effectively monitoring pasture-based livestock production systems. Remote sensing provides a feasible alternative, featuring a variety of techniques for FM estimation (Clementini et al., 2020; Chen et al., 2021). Regression models were among the earliest methodologies employed for estimating FM. Schaefer and Lamb (2016) employed regression analysis to field NDVI and LiDAR data to improve pasture biomass estimation. Sibanda et al. (2016) compared FM estimation in fertilized and unfertilized grass plots using hyperspectral data resampled to Sentinel-2 Multispectral Imager (MSI) and Landsat 8 Operational Land Imager (OLI) resolutions. Schucknecht et al. (2017) mapped rangeland FM production using Moderate Resolution Imaging Spectroradiometer (MODIS) phenology-based cumulative NDVI. Batistoti et al. (2019) employed a regression analysis with field and unmanned aerial vehicle (UAV) data. Amies et al. (2021) produced a national pasture productivity map for New Zealand using Sentinel-2 imagery and field measurements, developing a regression model with NDVI.

Mechanistic and dynamic models simulate the impacts of different management practices on pasture production and estimate pasture growth and nutritive value based on real-time soil, plant, and weather conditions. Silva et al. (2022) validated the DayCent process-based model for a typical Integrated Crop-Livestock System in Brazil from 2018 to 2020. Xie et al. (2022) developed a novel physically-based method for estimating aboveground biomass (AGB) using PROSAIL model inversion. Santos et al. (2024) employed the CROPGRO Perennial Forage Model to estimate pasture primary production for a yield gap analysis of pasture-based beef cattle production in Brazil. Bender et al. (2024) developed a new forage module within the ECOSystem Model Simulator, tested under continuous and rotational stocking methods. This module, which considers both grazing and cutting regimes, was used to assess its performance in simulating forage dynamics under different management scenarios.

FM estimation has been explored in the context of machine learning (ML) applications. Reis et al. (2020) evaluated the use of spectral and textural data from PlanetScope imagery for FM estimation and monitoring. Chen et al. (2021) developed a sequential neural network that integrates Sentinel-2 time-series data, field biomass observations, and climate variables. Rosa et al. (2021) tested an integrated method by combining UAV-acquired multispectral imagery, statistical models, and ML to predict pasture biomass. Freitas et al. (2022) explored the use of multispectral bands, vegetation indices, and Gray-Level Cooccurrence Matrix (GLCM) textures to estimate pasture FM using Random Forest (RF) classifier. Defalque et al. (2024) designed ML models to estimate biomass and dry matter from *Brachiaria brizantha* cv. Marandu pastures.

ML algorithms have increasingly focused on novel metaheuristic optimization algorithms inspired on nature or social behaviors. These

approaches improve optimization tasks by balancing exploration and exploitation, demonstrating superior performance over traditional methods in solving complex problems. The common thread among these methods is their application of bio-inspired mechanisms to optimization in ML and other computational fields. El-kenawy et al. (2024a) explored a new metaheuristic optimization method in ML and proposed an algorithm that improves the efficiency of problem solving. Abdollahzadeh et al. (2024) presented the Puma optimizer, inspired by the behavior of pumas, which improves optimization tasks in ML applications. El-Kenawy et al. (2024b) introduced the Football Optimization Algorithm, which exploits the dynamics of football teams to solve optimization problems more effectively than other algorithms.

This study explores a novel approach that integrates multi-sensor orbital imagery with agrometeorological modeling. We hypothesize that this integration will enable accurate and reliable FM estimation, thereby improving the monitoring of pasture-based livestock production systems. The objective of this study is to develop a replicable methodology for estimating FM using multi-sensor satellite data. Specifically, we applied the Simple Algorithm for Evapotranspiration Retrieving (SAFER), Monteith's Light Use Efficiency (LUE) model, NASA Harmonized Landsat and Sentinel-2 (HLS) surface reflectance imagery, and climate data to estimate FM for three pasture-based livestock production systems during both dry and rainy seasons.

2. Materials and methods

2.1. Study area

This study was conducted at the Brazilian Agricultural Research Corporation Southeast Livestock Center (Embrapa Pecuária Sudeste), located in the municipality of São Carlos, Brazil (latitude: 21° 57' S; longitude: 47° 50' W; elevation: 860 m) (Fig. 1). Its historical importance in the Brazilian agricultural research, especially in the livestock sector, can be highlighted by several key factors. For example, Brazilian Agricultural Research Corporation Southeast Livestock Center was the birthplace of the Canchim cattle breed, a milestone in the Brazilian livestock breeding. Its geographical location in the transition region between the Cerrado and Atlantic Forest biomes provides a unique opportunity to study the interactions between livestock production and environmental dynamics. These biomes, which support extensive pastures, further increase the relevance of the region for livestock research.

The climate is classified as tropical highland (Cwa), characterized by a temperate or subtropical hot summer with two distinct seasons. The rainy season extends from October to March, with an average temperature of 23.0 °C and average precipitation of 1100 mm. The dry season extends from April to September, with an average temperature of 19.9 °C and average precipitation of 250 mm. The dominant soil type is the dystrophic Red-Yellow Oxisol with a medium clay texture (Pezzopane et al., 2019; Vinholis et al., 2021).

The assessed pastured-based production systems varied in their management practices and land use strategies. The extensive (EXT)

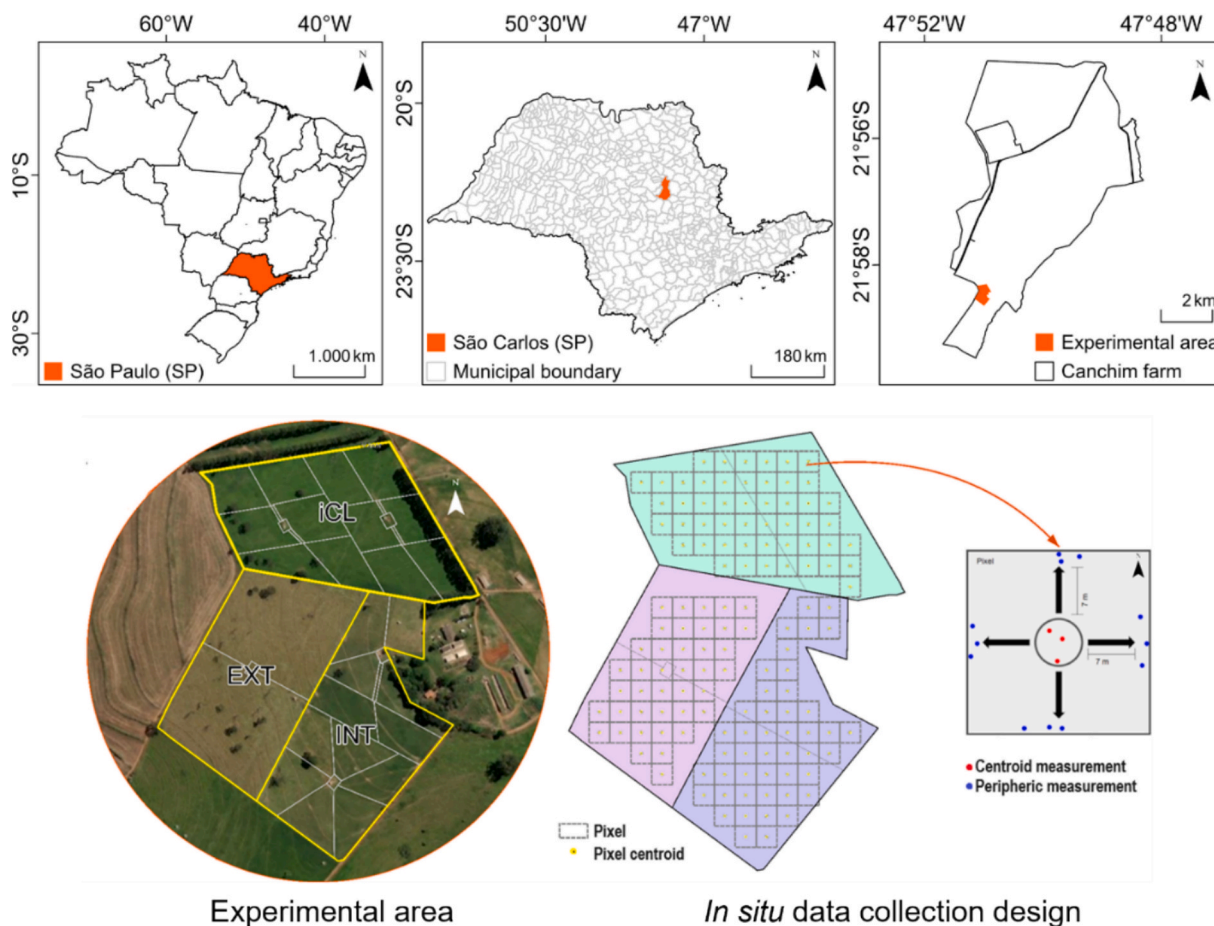


Fig. 1. Location of the pasture-based livestock production systems assessed in the experimental area, including the extensive production system (EXT), intensive production system (INT), and integrated crop-livestock (ICL) production system. This figure also shows the in-situ data collection design for each production system. Source: adapted from Bayma-Silva et al. (2019).

system involves continuous stocking, where livestock are allowed to graze freely over large areas without rotation. It is typically characterized by low stocking densities and minimal inputs in terms of fertilization and pasture management (Oliveira et al., 2020). In contrast, the intensive (INT) system uses rotational stocking, where animals are moved between paddocks in a controlled manner. This system typically involves higher stocking densities, aiming to optimize forage utilization and improve pasture quality through regular rotation and chemical fertilization (Balbino et al., 2011; Baronti et al., 2022). The integrated crop-livestock (ICL) system combines rotation, intercropping, or succession of crop and livestock activities within the same area. Pasture is managed with crop rotation and grazed using rotational stocking. The ICL system aims to boost productivity by alternating between crop production and livestock grazing, promoting synergies between the two components (Balbino et al., 2011; Vinhols et al., 2021; Soares et al., 2024).

In the study area, the 24-year-old EXT production system does not use liming nor chemical fertilization and is planted with *Urochloa* (syn. *Brachiaria*) *decumbens* (Stapf) R. Webster. The INT production system, established in 2010, uses chemical fertilization and employs *Piatã* palisade grass (*Urochloa* *brizantha* (Hochst ex A. Rich.) Stapf cv. BRS *Piatã*). The ICL production system incorporates pasture with maize rotation. This system was also established in 2010. Each production system consisted of two contiguous plots of approximately 3 ha each. The INT and ICL plots were divided into six paddocks of 0.5 ha each. Details of the pasture production system management are shown in the [Supplementary Material 1](#).

In the INT and ICL production systems, pasture management involved chemical fertilization during the rainy season and forage supplementation during the dry season. In late 2017 and early 2018, two paddocks within each ICL production system were cultivated with maize for silage, while the remaining paddocks were grazed under rotational stocking with 9 days of occupancy followed by 27 days without occupancy. After maize harvest, the paddocks were grazed under a rotational stocking regime with 6 days of occupancy and 30 days without occupancy. Additional details on pasture production system management can be found in [Bayma-Silva et al. \(2019\)](#).

2.2. *In situ* forage mass collection and laboratory analysis

We measured FM using the indirect double sampling method as outlined by [Wilm et al. \(1944\)](#) and applied by [Silva et al. \(2020a\)](#), [Cezimbra et al. \(2021\)](#), [Bretas et al. \(2023\)](#), and [Bender et al. \(2024\)](#). In our study, FM refers to the total dry mass or weight of forage present per unit area above ground level ([Pedreira, 2002](#); [Costa et al., 2017](#); [Almeida et al., 2023](#)). This method combines canopy height measurements with destructive FM sampling. Two key procedures were implemented: field teams were instructed to exclude inflorescences in height measurements, and continuous stocking was evaluated across different phases of rotational stocking (grazing, pre-grazing, post-grazing, and growing) on a bimonthly basis for regression analysis between height and FM.

Sampling points for canopy height measurements were planned based on a pixel grid derived from HLS satellite images (30 m × 30 m). The grid was established according to the spatial resolution of the satellite imagery used in this study to accurately capture the spatial variability of the pasture within each pixel of the evaluated production system.

The pixel centroids were marked with numbered wooden stakes, placed by triangulation using known distances from a digital planimetric map of the study area. For each projected pixel, we took 15 canopy height measurements, three at the center of the pixel and 12 at peripheral regions, spaced 7 m from the center in the north, south, east, and west directions ([Fig. 1](#)). The decision to collect 15 height measurements per pixel ensures a comprehensive representation of the height distribution, accounts for spatial heterogeneity, and increases the

reliability of the regression model for FM estimation.

We collected data within the pixel area, even if it extended beyond the paddock boundary. Heights were measured using a quadrant ruler and an acetate sheet, known as uncompressed height. We recorded the pasture height at the point where the acetate sheet was suspended from the canopy.

We estimated field FM from canopy height measurements using equations calibrated every two months to account for spatio-temporal variations, as canopy structure (height and FM) varies with the phenological stage of the plants. Homogeneous regions within each paddock, characterized by low, medium, and high pasture canopy heights, were selected for destructive forage sampling.

We collected ten samples per paddock in the EXT production system and three samples per paddock in the INT production system for each canopy height group. In the EXT production system, sampling was conducted in one paddock, while in the INT production system, one paddock was sampled from each grazing phase (pre-grazing, grazing, post-grazing, and growing). The ICL production system was not sampled as it used the same forage species and rotational stocking strategies as the INT production system.

We used a 0.25 m² quadrat for sampling. Canopy height was measured as previously described, and the samples within the quadrat were cut at ground level and weighed to determine total fresh mass (TFM). A subsample of the TFM (aliquot 1) was placed in a circulating air oven at 65 °C for 72 h to estimate total dry mass (TDM). Additionally, we separated a second subsample (aliquot 2) from each canopy height class into leaf blades and sheath/stem, referred to as green mass (GM) and dead mass (DM), respectively. Each fraction was weighed, dried, and reweighed. We applied the proportions of leaves, stems, and dead material obtained from the second aliquot to the TDM value per hectare to estimate the production of these fractions. Further details on *in situ* forage mass collection can be found in [Bayma-Silva et al., 2019](#).

GM represents the actively growing, photosynthetically efficient portion of the forage, which is the most nutritious component of the animal's diet. It is a more accurate indicator of pasture availability and quality, characterized by high protein content, digestibility and intake, and contributes to grass adaptation to grazing and tolerance to cutting ([Wilson and Mannetje, 1978](#); [Sousa-Baracho et al., 2024](#)). This focus ensures better estimates of livestock nutrition, grazing capacity, and overall pasture productivity. GM was correlated with the SAFER model, which estimates biophysical parameters based on the NDVI ([Rouse et al., 1974](#)). NDVI is effective for correlating field measurements of forage mass with SAFER model estimates due to its high sensitivity to leaf chlorophyll content.

Measurements were taken on a 32-day cycle, providing data on GM in kg ha⁻¹ month⁻¹. The frequency of FM collection was aligned with the forage growth cycle, covering the pre-grazing, grazing, and post-grazing phases in intensive systems to capture the dynamic changes in forage availability over time ([Nogueira et al., 2022](#)). However, data were not gathered in January and June 2018 and February and November 2019 due to operational issues ([Table 1](#)).

2.3. Modelling green mass (GM)

We applied the SAFER model, combined with Monteith's LUE model ([Monteith, 1972](#)), to estimate FM, offering several significant advantages. A primary benefit of SAFER is that it does not require a thermal band, which allows for the use of a wider range of sensors without this band. Moreover, SAFER can be applied with data from various types of stations (agrometeorological, conventional, and automatic) without needing crop classification data or complex radiation physics. This flexibility is especially valuable for analyzing historical trends in energy balance components and large-scale water productivity over time, as it increases the volume of available data for processing. This is crucial given that automatic sensors correspond to a relatively recent technological advancement ([Teixeira et al., 2013](#)). [Subhashree et al. \(2023\)](#)

Table 1
Canopy height measurement and forage mass sampling schedule.

Year	Jan	Feb	Mar	Apr	May	Jun	Jul	Aug	Sept	Oct	Nov	Dec
2018	–	8	14	16	17	–	20	21	21	24	26	27
2019	28	–	18	2	3	6	8	8	9	10	13	–

identified a research gap in incorporating climate data for predicting FM.

The SAFER model is based on the modeled ratio of actual evapotranspiration (ET_a) and reference evapotranspiration (ET_0). It was developed and validated in Brazil using field data from four flux stations and Landsat imagery (Teixeira et al., 2013). The SAFER model has been widely used to estimate biophysical parameters of different types of land use and land cover classes, including pasture (Bayma-Silva et al., 2016), croplands (Leivas et al., 2015; Rampazo et al., 2021), and water productivity (Teixeira et al., 2021).

The SAFER model estimates biomass using both climatic parameters and remote sensing-derived inputs, as described by Teixeira (2010) and Teixeira et al. (2013). It requires surface reflectance and climate data as inputs. Surface reflectance data were obtained from NASA's HLS project, which provides a consistent surface reflectance dataset acquired by the OLI and MSI sensors on board the Landsat 8 and Sentinel-2 satellites, respectively (Masek et al., 2021). This virtual constellation provides global coverage within a 30-meter resolution every 2 – 4 days. The project's primary goal is to generate consistent time series observations for monitoring land surface changes (Claverie et al., 2018).

The HLS products employ the following processing steps: (i) spatial co-registration, performed using the Automated Registration and Orthorectification Package; (ii) atmospheric correction, applied using the Land Surface Reflectance Code (Vermote et al., 2016), which is based on the 6S radiative transfer model and validated through the CEOS Atmospheric Correction Inter-Comparison Exercise (ACIX) I and II initiatives (Doxani et al., 2018, 2023); (iii) cloud masking, generated by the F-mask algorithm (Zhu et al., 2015); (iv) view and illumination angle normalization, conducted using the c-factor global 12-month fixed bidirectional reflectance distribution function (BRDF) technique (Roy et al., 2017); and (v) bandpass adjustment, achieved through a linear fit between equivalent spectral bands, with OLI spectral bands serving as a reference for adjusting MSI spectral bands.

The HLS suite includes three products: S10, a MSI surface reflectance at native resolutions (10 m, 20 m, and 60 m); S30, a MSI harmonized surface reflectance resampled to 30 m and matched to the Landsat 8 spectral response function; and L30, an OLI harmonized surface reflectance and top-of-atmosphere (TOA) brightness temperature resampled to 30 m in the Sentinel-2 tiling system. This product has been used in various studies, including vegetation classification (Ju and Bohrer, 2022); daily evapotranspiration estimate (Xue et al., 2021), cropland abandonment analysis (Hong et al., 2023), and studies on savanna and pasture areas (Parreiras et al., 2025).

In this study, we selected the L30 and S30 Version 1.4 products from February 2018 to November 2019 to construct surface reflectance time series. The HLS time series was built using cloud-free images acquired concomitant with the field campaign dates. However, it was not possible to obtain images near field campaign date in November 2018 due to cloud cover (Table 2).

Input climate parameters included global solar radiation (R_G), air temperature (T), and reference evapotranspiration (ET_r), which were derived from maximum and minimum temperatures, relative humidity

Table 2
HLS dataset image acquisition schedule.

Year	Jan	Feb	Mar	Apr	May	Jun	Jul	Aug	Sept	Oct	Nov	Dec
2018	–	9	16	20	15	–	19	21	22	22	–	6/31
2019	28	–	17	2	5	4	9	8	9	11	11	–

(maximum and minimum), and wind speed, following the Monteith radiation model (Monteith, 1972). The climatic data were obtained from an agrometeorological station located adjacent to the experimental area (World Meteorological Organization's code: 86845).

We selected the HLS surface reflectance bands from the visible, red-edge, near-infrared (NIR), and shortwave infrared (SWIR) to calculate broadband, top-of-atmosphere planetary albedo (α_{TOA}), as described by Teixeira et al. (2013). We computed the normalized difference ratio between near-infrared (ρ_{NIR}) and red (ρ_{RED}) (Rouse et al., 1974). The surface temperature (T_s) was obtained as a residual in the radiation balance. The SAFER model was executed using the Model Builder function available in ESRI's ArcMap 10.0 software (Nuñez, 2017). The atmospheric correction was applied to the α_{TOA} data to derive surface albedo (α_0) (Eq. (1)):

$$\alpha_0 = 0.61 \times \alpha_{TOA} + 0.08 \quad (1)$$

The NDVI was calculated using the reflectance values of the red (ρ_{red}) and near infrared (ρ_{NIR}) bands from HLS images (Rouse et al., 1974) (Eq. (2)).

$$NDVI = \frac{(\rho_{NIR} - \rho_{red})}{(\rho_{NIR} + \rho_{red})} \quad (2)$$

The SAFER algorithm was applied with the Monteith's LUE model to estimate biomass. Teixeira (2009) utilized the Monteith radiation model (Monteith, 1972) for biomass estimation. We calculated the ratio between actual evapotranspiration and reference evapotranspiration (ET_a/ET_0) as shown in Eq. (3):

$$\left(\frac{ET_a}{ET_0}\right)_{SAFER} = \left\{ \exp \left[1.8 - 0.008 \times \left(\frac{T_0}{\alpha_0 \times NDVI} \right) \right] \right\} \frac{ET_{0annual}}{5} \quad (3)$$

where: $ET_{0annual}/5$ is the correction factor when there is no local calibration of the SAFER algorithm and $ET_{0annual}$ is the average annual reference evapotranspiration of the study site.

The actual evapotranspiration (ET_a , mm d⁻¹) was obtained according to Teixeira et al. (2015) (Eq. (4)):

$$ET_a = ET_0 \times \left(\frac{ET_a}{ET_0}\right)_{SAFER} \quad (4)$$

Absorbed photosynthetically active radiation (APAR) was directly estimated as a fraction of the photosynthetically active radiation (fPAR), which depends on NDVI and PAR, itself derived as a fraction of global radiation (Teixeira et al., 2015) (Eq. (5)):

$$APAR = (1.26 \times NDVI - 0.16) \times (0.44 \times R_G) \quad (5)$$

We calculated biomass (BIO), also referred to as green mass (GM), as the dry matter production per unit area over time using Monteith's radiation model (Eq. (6)):

$$BIO = 0.864 \times \epsilon_{max} \times E_f \times APAR \quad (6)$$

where: ϵ_{max} is the maximum efficiency in the use of radiation (3.0 for pastures) (Bastiaanssen and Ali, 2003); E_f is the evaporative fraction;

and APAR (Eq. (5)) is the absorbed photosynthetically active radiation (W m^{-2}).

2.4. SAFER model performance evaluation

In the experimental area, the methodology allowed the estimation of available FM every 32 days, taking into consideration the phases of rotational stocking (grazing, pre-grazing, post-grazing, and regrowth). The SAFER model was used to estimate daily GM. This daily GM was then multiplied by the number of growth days in a given month, with pasture growth days defined as the interval between cattle removal and their return to the same paddock.

The FM available per hectare every 32 days was compared with the monthly accumulated GM per hectare estimated by the SAFER model. We combined satellite-based parameters with field observations to develop regression models for estimating GM more effectively. Regression analysis is widely used in biomass estimation due to its effectiveness and simplicity (Chen et al., 2021). Thus, it was chosen due to its reduced sample size demands, when compared with machine learning methods, and its suitability for the scale of the dataset, making regression analysis suitable approach in this context.

Initially, we applied ordinary least square regression and carried out a residual analysis to check for normality and homoscedasticity of the residuals. The residuals were considered normal and homoscedastic. To assess the uncertainty of this model, we used bootstrap resampling with

1001 interactions (Efron, 1992). The regression results were analyzed using the adjusted coefficient of determination (R_{adj}^2) and the root mean square error (RMSE). The results were reported with a 95 % confidence interval and statistical significance defined at $p < 0.05$.

3. Results and discussion

3.1. Seasonal dynamics of NDVI and climate data

The initial analysis focused on evaluating NDVI within pasture-based livestock production systems and climatic data. Fig. 2 presents the monthly average values of NDVI, global solar radiation (R_G), incident solar radiation at the top of the atmosphere (R_A), T_a , ET_o , and monthly cumulative precipitation of the study area.

NDVI and climate parameters exhibited strong seasonal variations, with lower values during the dry season (April to September) and higher values in the rainy season (October to March). NDVI values in 2018 were lower compared to 2019, especially during the rainy season. This trend is consistent with the ET_o values, as they are highly correlated (Alam et al., 2018). This pattern can be explained by the lower dry season precipitation in 2018 compared to 2019, with a total accumulation of 187.4 mm in 2018 versus 380.73 mm in 2019. This difference in dry season precipitation likely influenced the total rainfall at the beginning of the rainy season and consequently the NDVI values.

The mean NDVI values for the INT and ICL production systems were

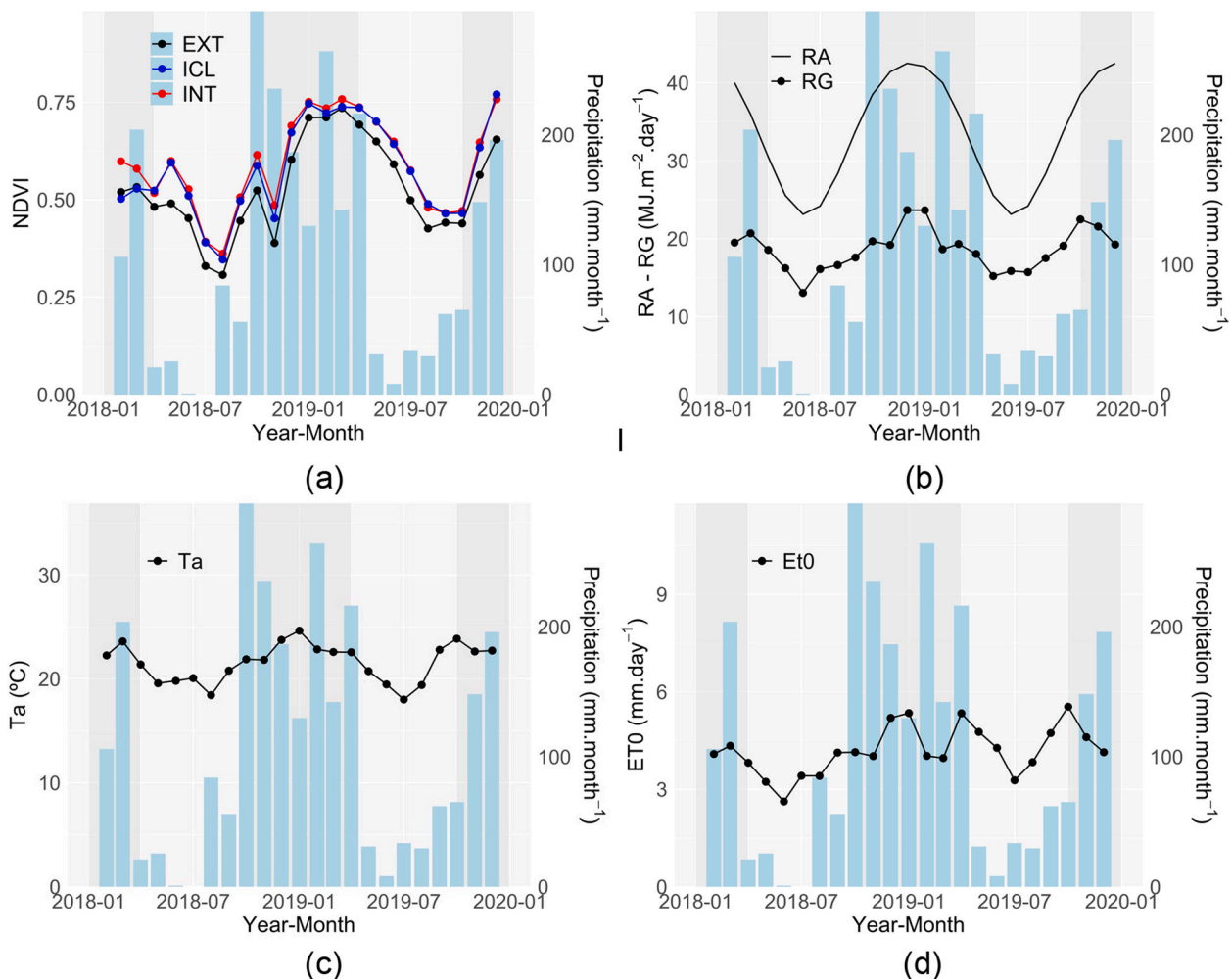


Fig. 2. Monthly average NDVI for extensive (EXT), intensive (INT), and intensive crop-livestock (ICL) production systems (a); solar radiation at the top of the atmosphere (R_A) and global solar radiation (R_G) (b), surface temperature (T_a) (c), and reference evapotranspiration (ET_o) (d) for the years 2018 and 2019. Light and dark gray areas represent the dry and rainy seasons, respectively.

0.574 and 0.583, respectively, which were slightly higher than the value for the EXT system (0.522). This difference can be attributed to the impacts of livestock rotation, supplementation, and forage fertilization, all of which contribute to improved forage health and productivity in intensive production systems. These results are consistent with Blanco et al. (2009), who reported similar results when they compared NDVI data derived from the Landsat Thematic Mapper (TM) images from extensive and intensive (rotational) livestock production systems in Argentina. Furthermore, Bayma-Silva et al. (2016) applied the SAFER model to Landsat 8 imagery to estimate forage biophysical parameters and found that intensive (rotational) systems exhibited higher NDVI values compared to extensive systems.

3.2. Time series analysis of field green mass (GM)

In the analysis of the field GM time series, the INT production system showed high GM values over the two-year period, averaging $1712 \pm 885 \text{ kg ha}^{-1}$ per month. Within this system, GM values reached $1804 \pm 848 \text{ kg ha}^{-1}$ per month during the rainy season and $1651 \pm 941 \text{ kg ha}^{-1}$ per month during the dry season. The ICL system presented an average GM of $1935 \pm 846 \text{ kg ha}^{-1}$ per month for the two-year period, $1953 \pm 882 \text{ kg ha}^{-1}$ per month in the rainy season, and $1922 \pm 857 \text{ kg ha}^{-1}$ per month in the dry season. The EXT system presented lower GM values, with an average of $1381 \pm 901 \text{ kg ha}^{-1}$ per month over the two-year period, $1427 \pm 752 \text{ kg ha}^{-1}$ per month in the rainy season, and $1346 \pm 1030 \text{ kg ha}$ per month in the dry season.

Over the two-year period, and across both the rainy and dry seasons, the field GM values for the EXT and ICL systems differed by 332 kg ha^{-1} per month, 377 kg ha^{-1} per month, and 304 kg ha^{-1} per month, respectively. These differences were higher when compared to the INT system, which showed variations of 555 kg ha^{-1} per month, 526 kg ha^{-1} per month, and 576 kg ha^{-1} per month for the two-year period, wet and dry seasons, respectively. The significant variation observed in field GM during the rainy season of 2018, compared to that from 2019, can likely be attributed to a two-fold increase in the animal stocking rate. In the rainy season of 2018, the stocking rate was 2.2 animal units per hectare, and it was reduced to 1.0 animal unit per hectare at the beginning of 2019.

As expected, intensive production systems exhibited higher field GM compared to the extensive production system, especially during the dry period (Fig. 3). This finding is consistent with observations obtained by Na et al. (2018), who reported that FM was higher in INT (rotational) grazing systems, compared to the EXT grazing areas. Similarly, Pezzopane et al. (2019) found that field FM was higher in INT systems compared to the EXT system in the same experimental area between 2013 and 2015. However, during the dry period, field FM was comparable with all pasture-based livestock production systems.

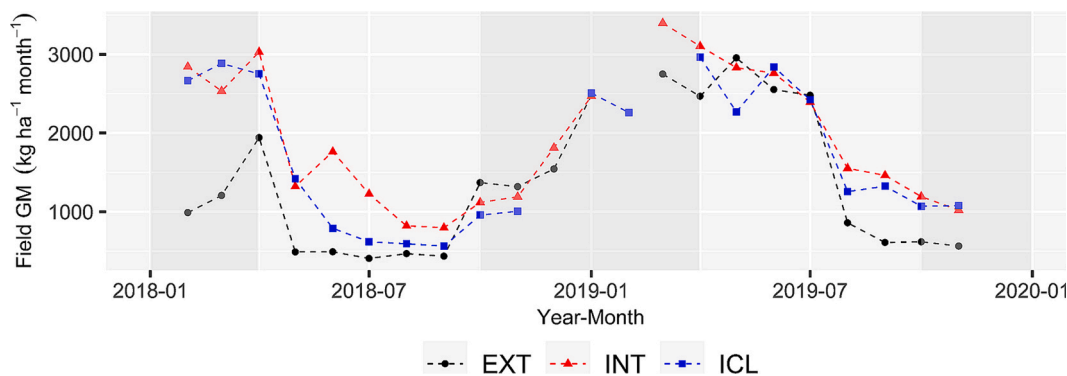


Fig. 3. Field green biomass (GM) in the evaluated pasture-based livestock production systems. FM = Forage mass; EXT = extensive production system; INT = intensive production system; and ICL = intensive crop-livestock production system. Light and dark gray areas represent the dry and rainy seasons, respectively. (For interpretation of the references to colour in this figure legend, the reader is referred to the web version of this article.)

3.3. Relationship between field green mass (GM) and NDVI in rainy and dry seasons

Linear regression analysis between field GM and NDVI for all pasture-based livestock production systems (Fig. 4) showed a positive correlation. However, only the EXT system exhibited an adjusted R^2 greater than 0.5. The ICL production system showed a weaker relationship between GM and NDVI ($R_{adj}^2 = 0.344$) compared to the INT production system ($R_{adj}^2 = 0.381$). This may be associated with FM variability resulting from the grazing frequency increased by crop integration within the ICL system. Grazing time within paddocks also contributed to greater variability in forage height and, consequently, all forage biophysical parameters. Grazing intensity has been identified as the most significant factor influencing forage mass dynamics (Numata et al., 2007).

In a study conducted by Reineremann et al. (2020), it was observed that NDVI was used as one of the model inputs in 62% of the 253 studies that examined pasture production through biomass sampling and remote sensing data. However, numerous studies have reported nonlinear relationships between NDVI and vegetation parameters, often due to NDVI saturation in densely vegetated areas (Huete et al., 1985; Yan et al., 2022). This saturation effect can reduce the accuracy of FM estimates based on NDVI, potentially leading to misestimations. This limitation arises from increased light interception within the canopy, which can introduce bias in NDVI values (Garrouette et al., 2016; Mutanga et al., 2023). Chen et al. (2021) observed that discrepancies between field FM measurements and NDVI values suggest that NDVI alone may not provide a direct and reliable estimates of FM.

3.4. Relationship between field green mass (GM) and accumulated SAFER green mass (GM) in dry and rainy seasons

The two-year comparative analysis, covering both rainy and dry seasons, showed significant relationships between field GM and accumulated GM estimates from the SAFER model across all three pasture-based livestock production systems. The SAFER model proved to be a strong positive predictor of field data, with R_{adj}^2 values ranging from 0.765 to 1.078 ($p < 0.001$ for all cases). The models accounted for a substantial proportion of the variance in the field data, with R_{adj}^2 values ranging from 0.670 to 0.856. The RMSE values indicated variability across all models, ranging from 342.4 to 485.9 kg ha^{-1} per month (Fig. 5).

The EXT production system provided the most accurate estimate ($R_{adj}^2 = 0.856$) and an RMSE of 342.4 kg ha^{-1} per month. In comparison, the ICL and INT production systems had lower R_{adj}^2 values (0.726 and 0.670, respectively) and higher RMSE values (ICL = 463.3 kg ha^{-1} per month; INT = 485.9 kg ha^{-1} per month). This can be explained to the higher need for intervention in forage, livestock and crop management. In

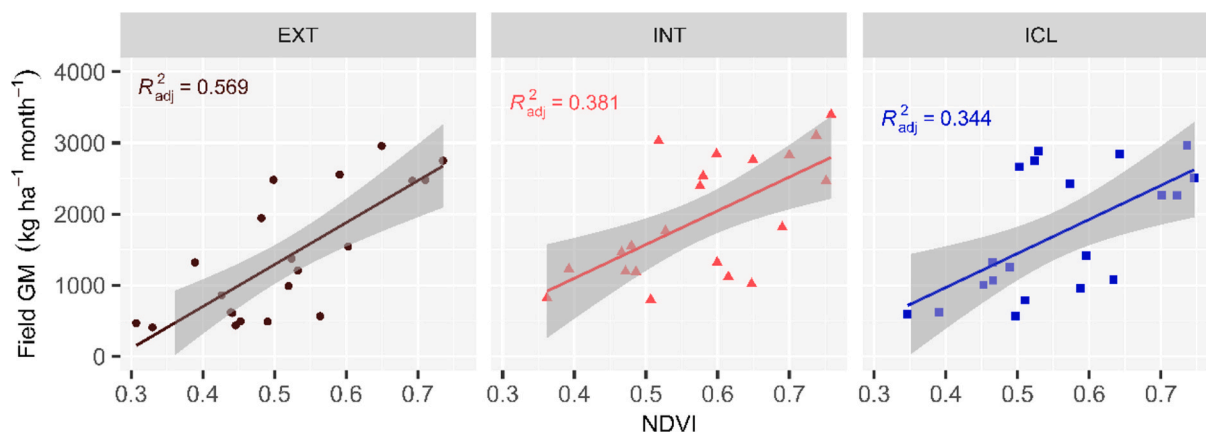


Fig. 4. Correlation between field green mass (GM) and NDVI in the evaluated livestock production systems. EXT = extensive production system; INT = intensive production system; and ICL = intensive crop-livestock production system. (For interpretation of the references to colour in this figure legend, the reader is referred to the web version of this article.)

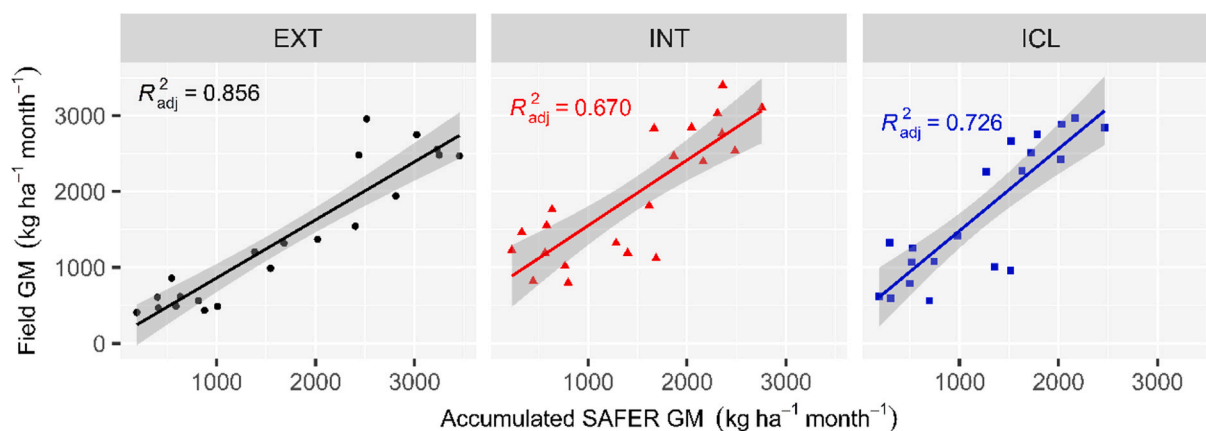


Fig. 5. Correlation between field green mass (GM) and accumulated SAFER green mass (GM) in the evaluated livestock production systems in dry and rainy seasons. (For interpretation of the references to colour in this figure legend, the reader is referred to the web version of this article.)

intensive systems, the rotation of livestock across different paddocks leads to increased variability in both forage height and mass availability (Hao et al., 2019; Cao et al., 2024).

Rosa et al. (2021) observed that the variability of post-grazing biomass was higher than that of pre-grazing pasture biomass in an intensive rotational farm. When comparing the results of the two intensive systems, we found that INT had lower performance. This result can be explained by the influence of cropping, as fertilization and crop residue decomposition improve soil quality and increase forage biomass (Silva et al., 2020; Fu et al., 2021).

The SAFER model demonstrated high performance in estimating GM for the EXT production system, with an R_{adj}^2 of 0.856 (ranging from 0.772 to 0.951). This performance was superior in comparison with previous models, including those developed by Anderson et al. (2017) (R^2 values varying from 0.62 to 0.77), Yang et al. (2018) (R^2 values between 0.75 and 0.85), Wang et al. (2019b) ($R^2 = 0.67$), Zeng et al. (2019) (R^2 from 0.69 to 0.86), and Amies et al. ($R^2 = 0.70$), demonstrating SAFER's superior accuracy.

The superior accuracy of the SAFER model in the EXT system can be attributed to its continuous stocking management approach, which results in a lower stocking rate, as shown in Supplementary Table 1. This reduced grazing pressure minimizes animal disturbance to the forage stand and canopy structure, promoting greater system stability. Consequently, reduced disturbance likely increases the consistency of vegetation conditions, improving the models predictive performance.

For the INT production system, the SAFER model achieved an R_{adj}^2 of

0.670, with a range between 0.456 and 0.830. This result is comparable to those reported by Chen et al. (2021) and Rosa et al. (2021), who obtained R^2 values of 0.6 and 0.68, respectively. It also outperformed the R^2 of 0.52 reported by Almeida et al. (2023), though it is lower than the value of 0.773 found by Defalque et al. (2024). The ICL production system presented an R_{adj}^2 of 0.726, with a range from 0.475 to 0.905, which also outperformed the models developed by Reis et al. (2020) ($R^2 = 0.65$), Silva et al. (2022) (R^2 ranging from 0.61 to 0.73), and Freitas et al. (2022) ($R^2 = 0.70$), demonstrating the superior accuracy of the SAFER model in estimating FM in an ICL production system.

Our findings are comparable to those reported in previous studies employing both regression analysis (Schmidt et al., 2016; Anderson et al., 2017; Amies et al., 2021; Almeida et al., 2023) and machine learning algorithms (Yang et al., 2018; Zeng et al., 2019; Reis et al., 2020; Chen et al., 2021; Rosa et al., 2021; Freitas et al. 2002). While regression models are site-specific, the SAFER model's performance is compatible with the state-of-the-art Machine Learning (ML) approaches, which utilize computational and statistical techniques for automated data analysis (Chen et al., 2021).

3.5. Relationship between field green mass (GM) and accumulated SAFER green mass (GM) in the dry and rainy seasons

The analysis of R_{adj}^2 values for the dry and rainy seasons indicated that the EXT production system consistently provided the most accurate estimates of FM. This system outperformed both the INT and ICL systems

in both dry and rainy seasons (Fig. 6). The linear regression analyses indicated a positive relationship between the field measurements and the SAFER model estimates. The data distribution was closer to the regression line during the dry season, compared to the rainy season, indicating that the models predictions were more precise in the dry season.

Previous studies have demonstrated that precipitation influences forage seed germination (Jongen et al., 2019), which may, in turn, affect forage productivity (Lai et al., 2022). Forage mass growth tends to decrease during the dry season, and root production is typically constrained by water availability (Wang et al., 2019a), negatively impacting forage mass production (Cao et al., 2024). The stability of forage mass during the dry season enhances model prediction, as it reduces variability and improves the accuracy of the estimates. In contrast, the wet season, characterized by rapid growth and dense forage, introduces complexities such as shadowing from the canopy layer (Barnetson et al., 2020).

In the dry season, regression analyses indicated significant positive relationships between the SAFER model estimates and field data for all three production systems. The SAFER model exhibited strong predictive power, with coefficients ranging from 0.769 to 1.078 ($p < 0.001$). The models explained substantial proportions of the variance in field data, with R^2_{adj} values ranging from 0.746 to 0.871. The RMSE values ranged from 338.7 to 431.3 kg ha^{-1} per month.

The SAFER model performed best in the ICL production system, achieving an R^2_{adj} of 0.871 (varying from 0.718 to 0.961), which was higher than the EXT system ($R^2_{adj} = 0.840$, ranging from 0.741 to 0.957)

and the INT system ($R^2_{adj} = 0.746$, ranging from 0.510 to 0.908). The ICL system also presented the lowest RMSE (305.5 kg ha^{-1} per month), compared to the EXT (367.4 kg ha^{-1} per month) and INT (400 kg ha^{-1} per month) systems.

Despite the limited literature on FM estimation during the dry season, our study's performance, with an R^2 of 0.746, surpasses previous such as those studies conducted by Punalekar et al. (2018) ($R^2 = 0.54$) and Legg and Bradley (2019) ($R^2 = 0.61$ – 0.75), which employed radiative transfer modelling with Sentinel-2 imagery and proximal ultrasound sonar, respectively.

In the rainy season, the SAFER model exhibited strong predictive power across all three production systems, with R^2_{adj} ranging from 0.795 for the EXT production system ($p < 0.001$), 1.106 for the INT ($p < 0.0068$), and 1.168 for the ICL system ($p < 0.0614$). Although the p -value of 0.0614 for the ICL system is marginally non-significant, the positive coefficient and the strong relationship observed in the other systems suggest a potential association between SAFER estimates and field data. However, due to the small sample size ($n = 8$) for the ICL system, caution must be considered in interpreting the results for this system.

The SAFER model showed the best performance in the EXT production system with an R^2_{adj} of 0.903 (ranging from 0.792 to 0.976), outperforming the INT system ($R^2_{adj} = 0.626$, ranging from 0.347 to 0.919) and the ICL system ($R^2_{adj} = 0.379$, ranging from -0.125 to 0.929). The RMSE values further reflect this performance, with the EXT achieving the lowest RMSE (196.1 kg ha^{-1} per month), compared to the INT (464.1 kg ha^{-1} per month) and ICL (576.4 kg ha^{-1} per month)

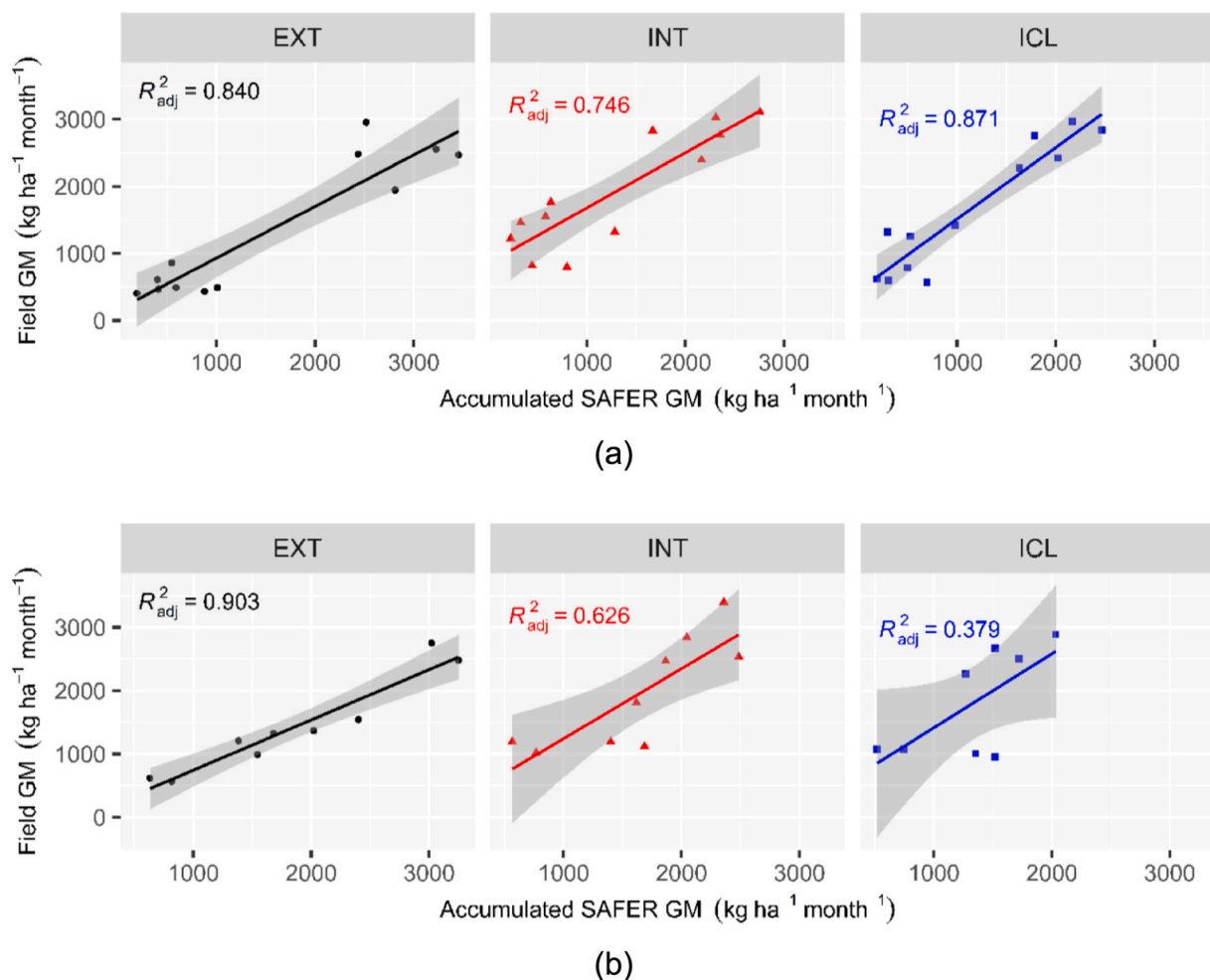


Fig. 6. Correlation between field green mass (GM) and accumulated SAFER green mass (GM) in the evaluated livestock production systems in the dry (a) and rainy (b) seasons. (For interpretation of the references to colour in this figure legend, the reader is referred to the web version of this article.)

systems.

Seasonal dynamics have important implications in livestock management. The main difference between the rainy and dry seasons lies in the increased attention required for forage and animal management during the dry season, mainly due to precipitation constraints. As detailed in the Supplementary Table 1, during the dry season (winter), supplemental feed was provided to the animals and paddock stocking rates were reduced to ensure optimal pasture utilization and maintain animal health. These seasonal dynamics highlight the importance of strategic adjustments in livestock management to preserve pasture quality and sustain animal productivity under more challenging conditions.

The SAFER model demonstrated higher predictive accuracy for the EXT production system when compared to other methodologies. Specifically, it outperformed the regression tree models of John et al. (2018) and the regression analysis of Schucknecht et al. (2017), both based on the 250-m spatial resolution, Moderate Resolution Imaging Spectroradiometer (MODIS) data, with their reported R^2 values of 0.68 and 0.47, respectively. The SAFER model achieved an R^2_{adj} of 0.903, evidencing its enhanced capability in capturing data variability and its suitability for individual farm applications, unlike the larger-scale approaches using MODIS data.

The use of Landsat 8 and Sentinel-2 data for analyzing pasture phenology, as noted by Wang et al. (2019b), demonstrated even higher accuracy. The combination of Landsat 8 and Sentinel-2 data achieved an

R^2 of 0.92, explaining more variation in phenological stages compared to MODIS data ($R^2 = 0.86$). This indicates that Landsat 8 and Sentinel-2, with finer spatial resolution (30 m and 10 m, respectively), offer better key pasture phenological phases.

Our results for the INT system were comparable to those results reported by Schaefer and Lamb (2016) and Crabbe et al. (2019). Specifically, the SAFER model achieved performance similar to that of Schaefer and Lamb (2016), who employed regression analysis on field and LiDAR data, obtaining an R^2 of 0.61. Likewise, our results were also aligned with Crabbe et al. (2019), who combined field and Sentinel-1 data with regression analysis, achieving an R^2 of 0.66. Nevertheless, in the rainy season, our results for the INT system did not reach the similar performance of Batistoti et al. (2019), who employed a regression analysis approach using field and UAV data, achieving a higher R^2 of 0.74.

The boxplots illustrate the model performance for EXT, INT, and ICL systems (Fig. 7). The EXT system consistently showed the highest R^2 and the lowest RMSE, indicating higher model accuracy. In contrast, both INT and ICL systems showed lower R^2 and higher RMSE, with greater variability and outliers, suggesting increased prediction uncertainty. These results highlight the model's superior reliability in extensive systems and the challenges it faces in more complex, integrated systems. Fig. 8 presents the GM time series values estimated from field data, SAFER and adjusted SAFER derived from the linear regression equations.

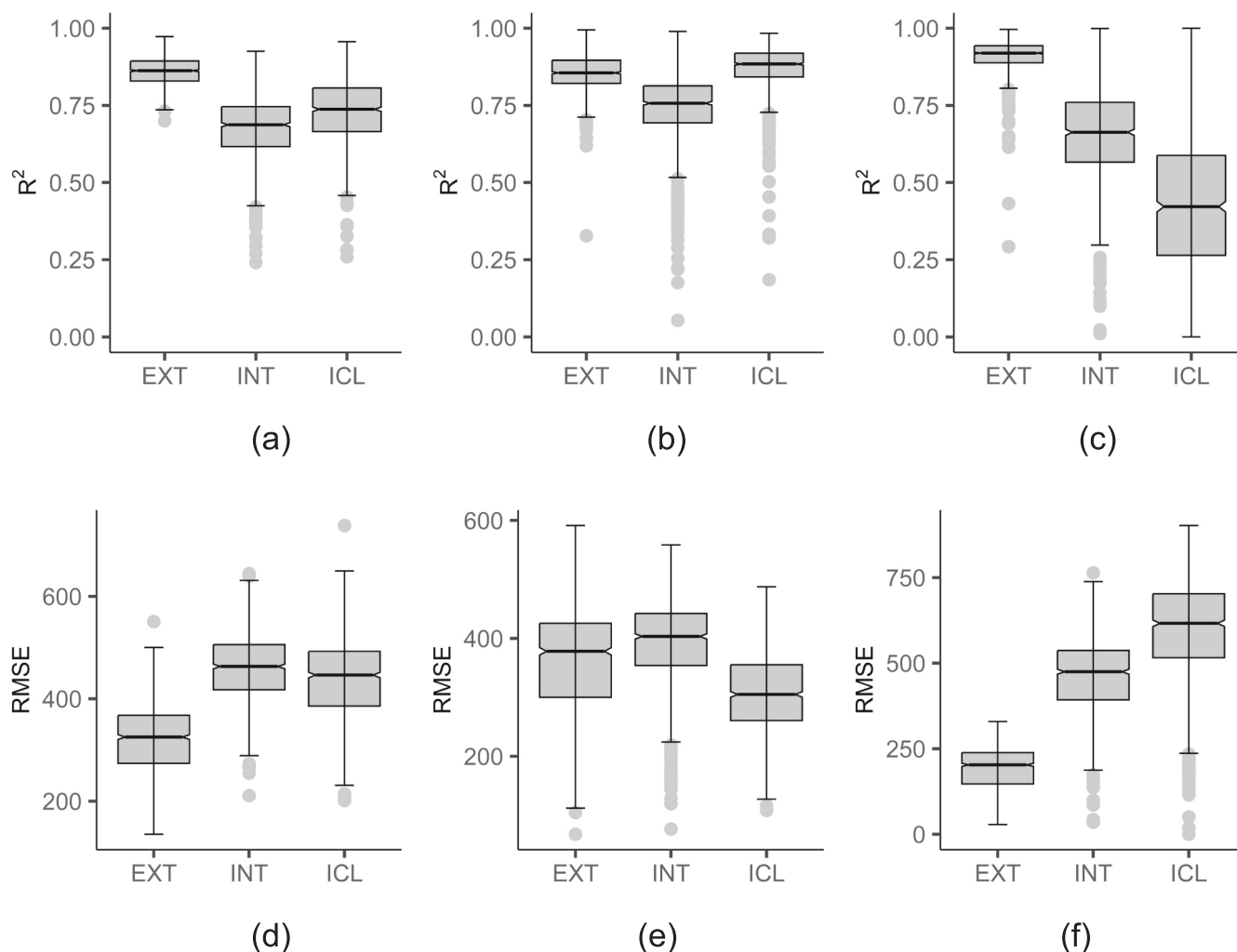


Fig. 7. R^2 results combining rainy and dry seasons (a), only from dry season (b), and only from rainy season (c); and RMSE results from rainy and dry season (d), only from dry season (e), and only from rainy season (f).

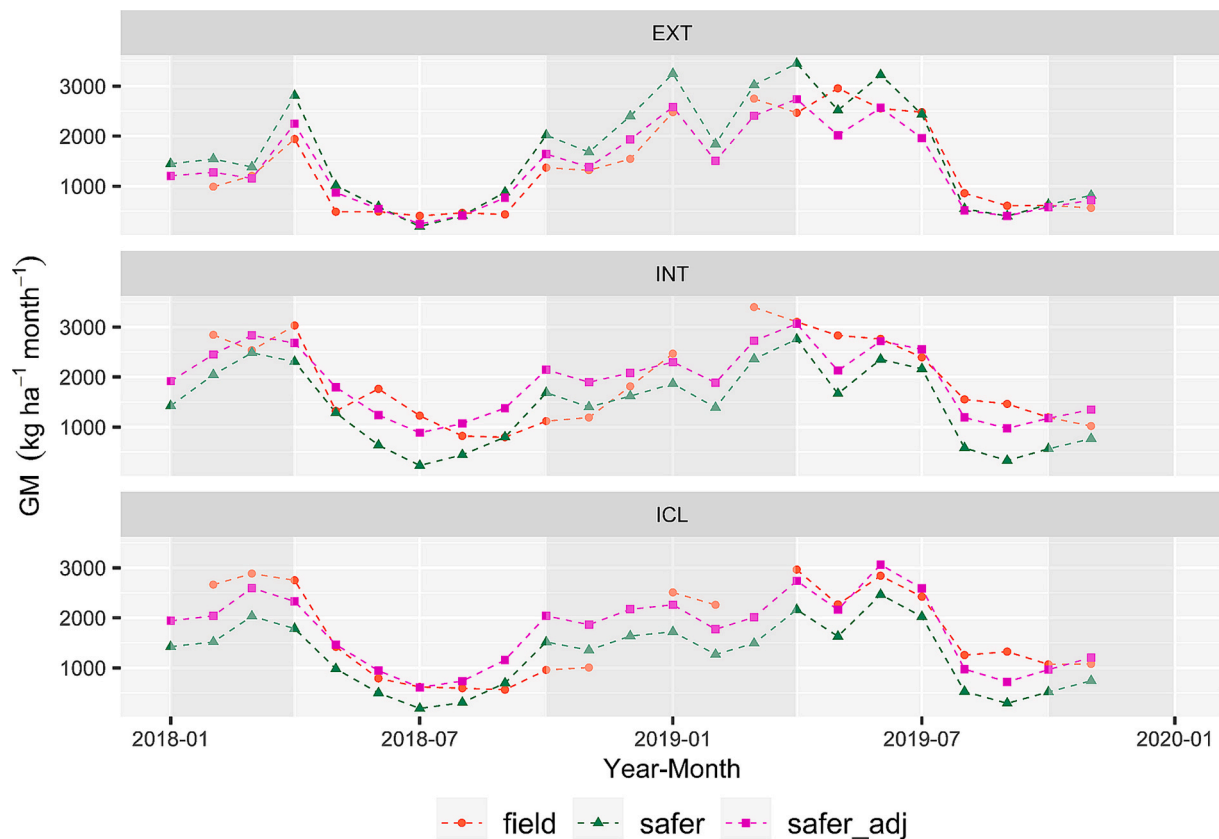


Fig. 8. Field, SAFER and adjusted SAFER (SAFER_adj) green mass (GM) time series in the evaluated livestock production systems. Light and dark gray areas represent the dry and rainy seasons, respectively.

3.6. Research limitations and managerial implications

Although remote sensing data are highly effective for monitoring large-scale land use and land cover change, their application to rangelands remains complex. Accurately distinguishing pasture from other land uses and differentiating between pasture production systems is a significant challenge (Bolfe et al., 2023). Shahi et al. (2025) identified spectral variability due to differences in livestock production and pasture management practices as a major limitation. As a result, satellite data may not effectively differentiate systems with similar spectral signatures, potentially leading to misclassification.

The SAFER model, while a valuable tool for estimating environmental parameters, does not incorporate biophysical soil properties or animal management data. As a result, it may not adequately capture the complex interactions among soil characteristics, grazing dynamics, and pasture growth that govern overall system performance. The omission of these factors constrains the model's ability to provide a comprehensive representation of FM in livestock production system dynamics.

The use of data from 2018–2019 may limit the applicability of the results to current conditions. Although more recent data were not available for this study, future research should prioritize integrating updated time series to improve the model's robustness and relevance. Expanding the temporal scope would provide a deeper understanding of how climate variability influences forage dynamics.

Furthermore, although the SAFER model has demonstrated its effectiveness in estimating forage mass under intensive management systems, its suitability to varying climatic conditions or pasture types, such as those with different species composition, degradation levels, and seasonality sensitivity, has yet to be evaluated. Addressing these limitations could improve the model's adaptability to different rangeland contexts and strengthen its contribution to broader monitoring efforts.

4. Conclusions

FM availability and quality are key determinants of stocking rates and livestock performance. Therefore, proper management is essential to prevent overgrazing, protecting rangeland ecosystems and supporting livelihoods. Maximizing the use of forage as a high-quality, cost-effective feed source is essential for a profitable pasture-based farm.

This study demonstrated the effectiveness of integrating multi-sensor satellite data with the SAFER agrometeorological model to estimate FM across three pasture-based livestock production systems in Brazil. The SAFER model explained over 67 % of FM variability, highlighting its potential as a scalable and automated tool for systematic pasture monitoring and data-driven grazing management. By incorporating remote sensing and climatic data, the SAFER model enhances FM estimation by accounting for differences in management intensity, pasture dynamics, and seasonal phenology throughout the year.

A key factor in achieving accurate FM estimates was distinguishing between GM and TDM. Unlike TDM, which includes senescent and indigestible plant material, GM is directly related to forage quality, livestock intake and overall pasture productivity. By prioritizing GM, the SAFER model produced more accurate estimates of available forage, enhancing its applicability for livestock nutrition, grazing capacity assessment, and pasture management.

The model performed best in the EXT system, where minimal management intervention led to more stable forage conditions and higher prediction accuracy. In intensive production systems, while SAFER also showed promising results for ICL systems, accuracy was slightly reduced in the INT system. In ICL systems, the influence of crop integration, such as fertilization and decomposition of crop residues, can improve soil quality and increase FM.

This research contributes to the development of systematic, automated, and repeatable methods for FM assessment, supporting improved

pasture monitoring and the formulation of optimized grazing strategies. The SAFER model, which uses accessible imagery and climate data, exhibits potential for application in tropical regions beyond Brazil. The widespread availability of input datasets facilitates the models adaptability in different geographical contexts. However, it is important to recognize that the accuracy of the model results depends heavily on the quality and accuracy of the input data, especially the climate data.

Future research could explore the use of higher resolution satellite imagery, such as the CBERS-4A and PlanetScope satellites to better capture spatial variability within paddocks. Additionally, increasing the frequency of field data collection by reducing the estimation interval from 32 days to 15 days, or even one week, may further improve FM estimation accuracy, particularly in intensive production systems.

CRedit authorship contribution statement

Gustavo Bayma: Writing – review & editing, Writing – original draft, Visualization, Validation, Supervision, Software, Resources, Project administration, Methodology, Investigation, Formal analysis, Data curation, Conceptualization. **Sandra Furlan Nogueira:** Writing – review & editing, Writing – original draft, Visualization, Validation, Supervision, Resources, Project administration, Methodology, Investigation, Funding acquisition, Formal analysis, Conceptualization. **Marcos Adami:** Writing – review & editing, Validation, Supervision, Software, Methodology, Investigation, Formal analysis, Data curation, Conceptualization. **Edson Eyji Sano:** Writing – review & editing, Validation, Supervision, Investigation, Formal analysis. **Daniel Coaguila Nuñez:** Writing – review & editing, Software, Methodology, Investigation, Data curation. **Patrícia Menezes Santos:** Writing – review & editing, Validation, Supervision, Resources, Project administration, Investigation, Funding acquisition. **José Ricardo Pezzopane:** Writing – review & editing, Validation, Investigation. **Célia Regina Grego:** Writing – review & editing, Validation, Investigation. **Antônio Heriberto de Castro Teixeira:** Writing – review & editing, Validation. **Sergii Skakun:** Writing – review & editing, Validation, Resources, Methodology.

Funding

This research was funded by “Animal Production in the Future: tools to support decision making in pasture management and transfer of technology” (Grant number 22.16.05.021.00.00) and “Carbon balance and footprint in soybean, corn, and sugarcane production: metrics, tools, and protocols for tropical and subtropical environments in the Brazilian territory” (Grant number 20.22.00.118.00.00).

Declaration of competing interest

The authors declare the following financial interests/personal relationships which may be considered as potential competing interests: Sandra Nogueira reports financial support was provided by Bayer Corporation Grant number 20.22.00.118.00.00. If there are other authors, they declare that they have no known competing financial interests or personal relationships that could have appeared to influence the work reported in this paper.

Acknowledgments

The authors would like to thank the field staff for their assistance and support during the fieldwork. We also acknowledge the important suggestions provided by the anonymous reviewers.

Data availability

The field data used in this study can be accessed at DOI: 10.48432/1VJD45. The SAFER ArcGIS Toolbox used in this study was developed

by Nuñez (2017) and will be made available on request.

Appendix A. Supplementary data

Supplementary data to this article can be found online at <https://doi.org/10.1016/j.compag.2025.110496>.

Data availability

Data will be made available on request.

References

- Abdollahzadeh, B., Khodadadi, N., Barshandeh, S., Trojovský, P., Gharehchopogh, F.S., El-kenawy, E.S.M., Abualgah, L., Mirjalili, S., 2024. Puma optimizer (PO): A novel metaheuristic optimization algorithm and its application in machine learning. *Clus. Comput.*, 27, 5235–5283. <https://doi.org/10.1007/s10586-023-04221-5>.
- Alam, M.S., Lamb, D.W., Rahman, M.M., 2018. A refined method for rapidly determining the relationship between canopy NDVI and the pasture evapotranspiration coefficient. *Comput. Electron. Agric.* 147, 12–17. <https://doi.org/10.1016/j.compag.2018.02.008>.
- Almeida, S.L.H., Souza, J.C., Nogueira, S.F., Pezzopane, J.R.M., Teixeira, A.H.C., Bosi, C., Adami, M., Zerbatto, C., Bernardi, A.C.C., Bayma, G., Silva, R.P., 2023. Forage mass estimation in silvopastoral and full sun systems: Evaluation through proximal remote sensing applied to the SAFER model. *Remote Sens.* 15, 815. <https://doi.org/10.3390/rs15030815>.
- Amies, A.C., Dymond, J.R., Shepherd, J.D., Pairman, D., Hoogendoorn, C., Sabetzade, M., Belliss, S.E., 2021. National mapping of New Zealand pasture productivity using temporal Sentinel-2 data. *Remote Sens.* 13, 1481. <https://doi.org/10.3390/rs13081481>.
- Andersson, K., Trotter, M., Robson, A., Schneider, D., Frizell, L., Saint, A., Lamb, D., Blore, C., 2017. Estimating pasture biomass with active optical sensors. *Adv. Anim. Biosci.* 8, 754–757. <https://doi.org/10.1017/S2040470017000838>.
- Aquilani, C., Confessore, A., Bozzi, R., Sirtori, F., Pugliese, C., 2022. Precision Livestock Farming technologies in pasture-based livestock systems. *Animal* 16, 100429. <https://doi.org/10.1016/j.animal.2021.100429>.
- Balbino, L.C., Barcellos, A.O., Stone, L.F. (Eds), 2011. Marco referencial: Integração lavoura-pecuária-floresta. Brasília, Brazil, Embrapa, 130 p. (in Portuguese).
- Barnetson, J., Phinn, S., Scarth, P., 2020. Estimating plant pasture biomass and quality from UAV imaging across Queensland's rangelands. *AgriEngineering* 2, 523–543. <https://doi.org/10.3390/agriengineering2040035>.
- Baronti, S., Ungaro, F., Maienza, A., Ugolini, F., Lagomarsino, A., Agnelli, A.E., Calzolari, C., Pisseri, F., Robbiati, G., Vaccari, F.P., 2022. Rotational pasture management to increase the sustainability of mountain livestock farms in the Alpine region. *Reg. Environ. Change* 22, 50. <https://doi.org/10.1007/s10113-022-01884-5>.
- Bastiaanssen, W.G.M., Ali, S., 2003. A new crop yield forecasting model based on satellite measurements applied across the Indus Basin. *Pakistan. Agric. Ecosyst. Environ.* 94, 321–340. [https://doi.org/10.1016/S0167-8809\(02\)00034-8](https://doi.org/10.1016/S0167-8809(02)00034-8).
- Batistoti, J., Marcatto, J., Itavo, L., Matsubara, E., Gomes, E., Oliveira, B., Souza, M., Siqueira, H., Filho, G.S., Akiyama, T., Gonçalves, W., Liesenberg, V., Li, J., Dias, A., 2019. Estimating pasture biomass and canopy height in Brazilian savanna using UAV photogrammetry. *Remote Sens.* 11, 2447. <https://doi.org/10.3390/rs11202447>.
- Bayma-Silva, G., Teixeira, A.H.C., Victoria, D.C., Nogueira, S.F., Leivas, J.F., Coaguila, D. N., Herling, V.R., 2016. Energy balance model applied to pasture experimental areas in São Paulo State, Brazil. *Proc. SPIE* 9998, Remote Sensing for Agriculture, Ecosystems, and Hydrology XVIII, 99981C. DOI: 10.1117/12.2242043.
- Bayma-Silva, G., Grego, C.R., Koenigkan, L.V., Nogueira, S.F., Pezzopane, J.R.M., Santos, R.C., Santos, P.M., Santos, T.T., Takemura, C.M., 2019. Protocolo de campo para investigação, calibração e validação de métodos para estimativa de massa de forragem baseados em sensoriamento remoto orbital e proximal. Campinas, Brazil, Embrapa Informática Agropecuária (Campinas, Comunicado Técnico, 133). Available at: <https://ainfo.cnptia.embrapa.br/digital/bitstream/item/207223/1/ComunicadoTecnico-133.pdf> Access 21 Apr. 2024 (in Portuguese).
- Bender, F.D., Cuadra, S.V., Dias, H.B., Silva, L.E.A., Oliveira, M.P.G., Lamparelli, R.A.C., Cabral, O.M.R., Nogueira, S.F., Pezzopane, J.R.M., Bosi, C., Freitas, H.C., Magalhães, P.S.G., 2024. A new perennial forage module coupled with the ECOSMOS terrestrial ecosystem model: Calibration and evaluation for Urochloa (syn. Brachiaria) brizantha. *Eur. J. Agron.*, 159, 127253. <https://doi.org/10.1016/j.eja.2024.127253>.
- Beukes, P.C., McCarthy, S., Wims, C.M., Gregorini, P., Romera, A.J., 2019. Regular estimates of herbage mass can improve profitability of pasture-based dairy systems. *Anim. Prod. Sci.* 59, 359–367. <https://doi.org/10.1071/AN17166>.
- Blanco, L.J., Ferrando, C.A., Biurrun, F.N., 2009. Remote sensing of spatial and temporal vegetation patterns in two grazing systems. *Rangel. Ecol. Manag.* 62, 445–451. <https://doi.org/10.2111/08-213.1>.
- Bolfe, E.L., Parreiras, T.C., Silva, L.A.P., Sano, E.E., Bettiol, G.M., Victoria, D.C., Sanches, I.D., Vicente, L.E., 2023. Mapping agricultural intensification in the Brazilian savanna: A machine learning approach using harmonized data from Landsat Sentinel-2. *ISPRS Int. J. Geo-Information* 12 (7), 263. <https://doi.org/10.3390/ijgi12070263>.
- Bretas, L.L., Dubeux Jr, J.C., Cruz, P.J., Queiroz, L.M., Ruiz-Moreno, M., Knight, C., Bernardini, M.A., 2023. Monitoring the effect of weed encroachment on cattle

- behavior in grazing systems using GPS tracking collars. *Animals* 13, 3353. <https://doi.org/10.3390/ani13213353>.
- Cao, F., Li, W., Jiang, Y., Gan, X., Zhao, C., Ma, J., 2024. Effects of grazing on grassland biomass and biodiversity: A global synthesis. *Field Crops Res.* 306, 109204. <https://doi.org/10.1016/j.fcr.2023.109204>.
- Capristo, D.P., Ceccon, G., Fachinelli, R., Tomazi, M., 2021. Microbiological and structural quality of Oxisol under pasture renewal systems. *Pesq. Agropecu. Trop.* 51, e68006. <https://doi.org/10.1590/1983-40632021v51e68006>.
- Carvalho, A.M., Santos, D.C.R., Ramos, M.L.G., Marchão, R.L., Vilela, L., Sousa, T.R., Malaquias, J.V., Gonçalves, A.D.M.A., Coser, T.R., Oliveira, A.D., 2022. Nitrous oxide emissions from a long-term integrated crop-livestock system with two levels of P and K fertilization. *Land* 11, 1535. <https://doi.org/10.3390/land11091535>.
- Castro, D., de Lima, D.A.C., Romano, C., 2022. The telecoupling approach to the global food system and climate change regime: The pivotal role of Brazil and China. *Environ. Clim. Smart Food Prod.* 73–107. https://doi.org/10.1007/978-3-030-71571-7_3.
- Cezimbra, I.M., Nunes, P.A.A., Souza Filho, W., Tischler, M.R., Genro, T.C.M., Bayer, C., Carvalho, P.C.F., 2021. Potential of grazing management to improve beef cattle production and mitigate methane emissions in native grasslands of the Pampa biome. *Sci. Total Environ.*, 780, 146582. <https://doi.org/10.1016/j.scitotenv.2021.146582>.
- Chen, Y., Guerschman, J., Shendryk, Y., Henry, D., Harrison, M.T., 2021. Estimating pasture biomass using Sentinel-2 imagery and machine learning. *Remote Sens.* 13, 603. <https://doi.org/10.3390/rs13040603>.
- Cheng, M., Quan, J., Yin, J., Liu, X., Yuan, Z., Ma, L., 2023. High-resolution maps of intensive and extensive livestock production in China. *Resour. Environ. Sustain.* 12, 100104. <https://doi.org/10.1016/j.resenv.2022.100104>.
- Claverie, M., Ju, J., Masek, J.G., Dungan, J.L., Vermote, E.F., Roger, J.C., Skakun, S.V., Justice, C., 2018. The Harmonized Landsat and Sentinel-2 surface reflectance data set. *Remote Sens. Environ.* 219, 145–161. <https://doi.org/10.1016/j.rse.2018.09.002>.
- Clementini, C., Pomente, A., Latini, D., Kanamaru, H., Vuolo, M.R., Heuroux, A., Fujisawa, M., Schiavon, G., Del Frate, F., 2020. Long-term grass biomass estimation of pastures from satellite data. *Remote Sens.*, 12, 2160. <https://doi.org/10.3390/rs12132160>.
- Costa, J.A.A. da, Queiroz, H.P. de, 2017. *Régua de Manejo de Pastagens: edição revisada*. Embrapa Gado de Corte, Folhetos. Available at: <https://ainfo.cnptia.embrapa.br/digital/bitstream/item/165094/1/Regua-de-manejo-de-pastagens.pdf>. Accessed 04 Feb 2025.
- Crabbe, R.A., Lamb, D.W., Edwards, C., Andersson, K., Schneider, D., 2019. A preliminary investigation of the potential of Sentinel-1 radar to estimate pasture biomass in a grazed pasture landscape. *Remote Sens.* 11, 872. <https://doi.org/10.3390/rs11070872>.
- Defalque, G., Santos, R., Bungenstab, D., Echeverria, D., Dias, A., Defalque, C., 2024. Machine learning models for dry matter and biomass estimates on cattle grazing systems. *Comput. Electron. Agric.*, 216, 108520. <https://doi.org/10.1016/j.compag.2023.108520>.
- Dias-Filho, M.B., 2017. *Degradação de pastagens. O que é e como evitar*. Embrapa Amazônia Oriental, Belém, Brazil, 2017, 19 p. (in Portuguese).
- Doxani, G., Vermote, E., Roger, J.C., Gascon, F., Adriaensens, S., Frantz, D., Vanhellemont, Q., 2018. Atmospheric correction inter-comparison exercise. *Remote Sens.* 10, 352. <https://doi.org/10.1016/j.rse.2022.113412>.
- Doxani, G., Vermote, E.F., Roger, J.C., Skakun, S., Gascon, F., Collison, A., Yin, F., 2023. Atmospheric correction inter-comparison exercise, ACIX-II land: An assessment of atmospheric correction processors for Landsat 8 and Sentinel-2 over land. *Remote Sens. Environ.* 285, 113412. <https://doi.org/10.1016/j.rse.2022.113412>.
- Efron, B., 1992. *Bootstrap methods: Another look at the Jackknife*. In: Kotz, S., Johnson, N.L. (Eds.), *Breakthroughs in Statistics*. Springer, New York, pp. 569–593.
- El-kenawy, E.S.M., Khodadadi, N., Mirjalili, S., Abdelhamid, A.A., Eid, M.M., Ibrahim, A., 2024a. Greylag goose optimization: nature-inspired optimization algorithm. *Expert Systems with Applications* 238, 122147. <https://doi.org/10.1016/j.eswa.2023.122147>.
- El-kenawy, E.S.M., Rizk, F.H., Zaki, A.M., Mohamed, M.E., Ibrahim, A., Abdelhamid, A.A., Khodadadi, N., Almetwally, E.M., Eid, M.M., 2024b. Football optimization algorithm (fboa): A novel metaheuristic inspired by team strategy dynamics. *J. Artif. Intell. Metaheuristics* 8, 21–38. <https://doi.org/10.54216/JAIM.080103>.
- FAO. Food and Agriculture Organization of the United Nations. FAOSTAT, 2023. <http://www.fao.org/faostat/eb/#data>. Access 25 Aug. 2024.
- Feltran-Barbieri, R., Féres, J.G., 2021. Degraded pastures in Brazil: Improving livestock production and forest restoration. *R. Soc. Open Sci.* 8, 201854. <https://doi.org/10.1098/rsos.201854>.
- Fraundorfer, M., 2022. *Global food production*. In: *Global Governance in the Age of the Anthropocene*. Springer International Publishing, Cham, pp. 161–201. <https://doi.org/10.1007/978-3-030-88156-6>.
- Freitas, R.G., Pereira, F.R.S., Reis, A.A., Magalhães, P.S.G., Figueiredo, G.K.D.A., Amaral, L.R., 2022. Estimating pasture aboveground biomass under an integrated crop-livestock system based on spectral and texture measures derived from UAV images. *Comput. Electron. Agric.* 198, 107122. <https://doi.org/10.1016/j.compag.2022.107122>.
- Fu, B., Chen, L., Huang, H., Qu, P., Wei, Z., 2021. Impacts of crop residues on soil health: a review. *Soil Syst.* 5, 164–173. <https://doi.org/10.1080/26395940.2021.1948354>.
- Gargiulo, J., Clark, C., Lyons, N., Veyrac, G., Beale, P., Garcia, S., 2020. Spatial and temporal pasture biomass estimation integrating electronic plate meter, Planet cubesats and Sentinel-2 satellite data. *Remote Sens.* 12, 3222. <https://doi.org/10.3390/rs12193222>.
- Garrouste, E., Hansen, A., Lawrence, R., 2016. Using NDVI and EVI to map spatiotemporal variation in the biomass and quality of forage for migratory elk in the Greater Yellowstone Ecosystem. *Remote Sens.* 8, 404. <https://doi.org/10.3390/rs8050404>.
- Hao, Y., He, Z., 2019. Effects of grazing patterns on grassland biomass and soil environments in China: A meta-analysis. *PLoS One* 14, e0215223. <https://doi.org/10.1371/journal.pone.0215223>.
- Herrero, M., Thornton, P.K., Mason-D'Croz, D., Palmer, J., Benton, T.G., Bodirsky, B.L., West, P.C., 2020. Innovation can accelerate the transition towards a sustainable food system. *Nat. Food.*, 1, 266–272. <https://doi.org/10.1038/s43016-020-0074-1>.
- Hong, C., Prishchepov, A.V., Jin, X., Han, B., Lin, J., Liu, J., Ren, J., Zhou, Y., 2023. The role of harmonized Landsat Sentinel-2 (HLS) products to reveal multiple trajectories and determinants of cropland abandonment in subtropical mountainous areas. *J. Environ. Manag.*, 336, 117621. <https://doi.org/10.1016/j.jenvman.2023.117621>.
- Huete, A.R., Jackson, R.D., Post, D.F., 1985. Spectral response of a plant canopy with different soil backgrounds. *Remote Sens. Environ.* 17, 37–53. [https://doi.org/10.1016/0034-4257\(85\)90111-7](https://doi.org/10.1016/0034-4257(85)90111-7).
- IBGE. Instituto Brasileiro de Geografia e Estatística. Censo agropecuário: resultados definitivos, 2017. Rio de Janeiro, Brazil, IBGE, 2019. Available at: https://biblioteca.ibge.gov.br/visualizacao/periodicos/3096/agro_2017_resultados_definitivos.pdf. Access: 05 May 2024 (in Portuguese).
- John, R., Chen, J., Giannico, V., Park, H., Xiao, J., Shirkey, G., Ouyang, Z., Shao, C., Laforteza, R., Qi, J., 2018. Grassland canopy cover and aboveground biomass in Mongolia and Inner Mongolia: Spatiotemporal estimates and controlling factors. *Remote Sens. Environ.* 213, 34–48. <https://doi.org/10.1016/j.rse.2018.05.002>.
- Jongen, M., Förster, A.C., Unger, S., 2019. Overwhelming effects of autumn-time drought during seedling establishment impair recovery potential in sown and semi-natural pastures in Portugal. *Plant Ecol.* 220, 183–197. <https://doi.org/10.1007/s11258-018-0869-4>.
- Ju, Y., Bohrer, G., 2022. Classification of wetland vegetation based on NDVI time series from the HLS dataset. *Remote Sens.* 14, 2107. <https://doi.org/10.3390/rs14092107>.
- Lai, X., Shen, Y., Wang, Z., Ma, J., Yang, X., Ma, L., 2022. Impact of precipitation variation on summer forage crop productivity and precipitation use efficiency in a semi-arid environment. *Eur. J. Agron.* 141, 126616. <https://doi.org/10.1016/j.eja.2022.126616>.
- Legg, M., Bradley, S., 2019. Ultrasonic arrays for remote sensing of pasture biomass. *Remote Sens.* 12, 111. <https://doi.org/10.3390/rs12010111>.
- Leivas, J. F., Teixeira, A. H. D. C., Andrade, R. G., Victoria, D. D. C., Bayma-Silva, G., Bolfe, E. L., 2015. Application of agrometeorological spectral model in rice area in southern Brazil. *Proc. SPIE* 9637, Remote Sensing for Agriculture, Ecosystems, and Hydrology XVII, 96372B DOI: 10.1117/12.2194571.
- Masek, J., Ju, J., Roger, J., Skakun, S., Vermote, E., Claverie, M., Dungan, J., Yin, Z., Freitag, B., Justice, C., 2021. HLS Operational Land Imager surface reflectance and TOA brightness daily global 30m v2.0. NASA EOSDIS Land Processes Distributed Active Archive Center. DOI: 10.5067/HLS/HL30.002. Access: 30 Oct. 2023.
- Monteith, J.L., 1972. Solar radiation and productivity in tropical ecosystems. *J. Appl. Ecol.* 9, 747–766. <https://doi.org/10.2307/2401901>.
- Mutanga, O., Masenyama, A., Sibanda, M., 2023. Spectral saturation in the remote sensing of high-density vegetation traits: A systematic review of progress, challenges, and prospects. *ISPRS J. Photogramm. Remote Sens.*, 198, 297–309. <https://doi.org/10.1016/j.isprsjprs.2023.03.010>.
- Na, Y., Li, J., Hoshino, B., Bao, S., Qin, F., Myagmartseren, P., 2018. Effects of different grazing systems on aboveground biomass and plant species dominance in typical Chinese and Mongolian steppes. *Sustain.* 10, 4753. <https://doi.org/10.3390/su10124753>.
- Nogueira, S.F., Bayma-Silva, G., Grego, C.R., Santos, P.M., Pezzopane, J.R.M., 2022. Forage mass production in integrated, extensive and intensive livestock systems in the central region of the State of São Paulo. *Redape V1*. <https://doi.org/10.48432/1VDJ45>.
- Numata, I., Roberts, D.A., Chadwick, O.A., Schimel, J., Sampaio, F.R., Leonidas, F.C., Soares, J.V., 2007. Characterization of pasture biophysical properties and the impact of grazing intensity using remotely sensed data. *Remote Sens. Environ.* 109, 314–327. <https://doi.org/10.1016/j.rse.2007.01.013>.
- Núñez, D.N.C., 2017. *Determinação da evapotranspiração com aplicação do algoritmo SAFER em imagens Landsat na escala de microbacia (Doctoral thesis in Agronomy)*. Brazil, Universidade Estadual Paulista, Ilha Solteira.
- Oliveira, J., Campbell, E.E., Lamparelli, R.A.C., Figueiredo, G.K.D.A., Soares, J.R., Jaiswal, D., Monteiro, L.A., Vianna, M.S., Lynd, L.R., Sheehan, J.J., 2020. Choosing pasture maps: An assessment of pasture land classification definitions and a case study of Brazil. *Int. J. Appl. Earth Obs. Geoinf.*, 93, 102205. <https://doi.org/10.1016/j.jag.2020.102205>.
- Parreiras, T.C., Bolfe, É.L., Pereira, P.R.M., Souza, A.M., Alves, V.F., 2025. Applications, challenges and perspectives for monitoring agricultural dynamics in the Brazilian savanna with multispectral remote sensing. *Remote Sens. Appl. Soc. Environ.*, 37, 101448. <https://doi.org/10.1016/j.rsae.2025.101448>.
- Pedreira, C.G.S. 2002. *Avanços metodológicos na avaliação de pastagens*. In: *Reunião Anual da Sociedade Brasileira de Zootecnia*, 39., 2002, Recife. Anais... Recife: Sociedade Brasileira de Zootecnia, p.100-150. Available at: <https://www.fcav.unesp.br/Home/departamentos/zootecnia/ANACLAUDIARUGGIERI/termospedreira.pdf>. Access 23 Aug. 2024 (in Portuguese).
- Pezzopane, J.R.M., Bernardi, A.C.C., Azenha, M.V., Oliveira, P.P.A., Bosi, C., Pedrosa, A. F., Esteves, S.N., 2019. Production and nutritive value of pastures in integrated livestock production systems: Shading and management effects. *Sci. Agric.* 77, 2020. <https://doi.org/10.1590/1678-992X-2018-0150>.
- Phukubye, K., Mutema, M., Buthelezi, N., Muchaonyerwa, P., Cerri, C., Chaplot, V., 2022. On the impact of grassland management on soil carbon stocks: a worldwide

- meta-analysis. *Geoderma Reg.* 28, e00479. <https://doi.org/10.1016/j.geodrs.2021.e00479>.
- Piipponen, J., Jalava, M., de Leeuw, J., Rizayeva, A., Godde, C., Cramer, G., Herrero, M., Kumm, M., 2022. Global trends in grassland carrying capacity and relative stocking density of livestock. *Glob. Chang. Biol.* 28, 4117–4132. <https://doi.org/10.1111/gcb.16174>.
- Place, S.E., 2024. Examining the role of ruminants in sustainable food systems. *Grass Forage Sci.* 79, 135–143. <https://doi.org/10.1111/gfs.12673>.
- Polidoro, J.C., Freitas, P.L., Hernani, L.C., Anjos, L.H.C., Rodrigues, R.A.R., Caesário, F. V., Andrade, A.G., Ribeiro, J.L., 2021. Potential impact of plans and policies based on the principles of conservation agriculture on the control of soil erosion in Brazil. *Land Degrad. Dev.* 32, 3457–3468. <https://doi.org/10.22541/au.158750264.42640167>.
- Punalekar, S.M., Verhoef, A., Quaipe, T.L., Humphries, D., Birmingham, L., Reynolds, C. K., 2018. Application of Sentinel-2A data for pasture biomass monitoring using a physically based radiative transfer model. *Remote Sens. Environ.* 218, 207–220. <https://doi.org/10.1016/j.rse.2018.09.028>.
- Rampazo, N.A.M., Picoli, M.C.A., Teixeira, A.H.C., Cavaliero, C.K.N., 2021. Water consumption modeling by coupling MODIS images and agrometeorological data for sugarcane crops. *Sugar Tech.* 23, 524–535. <https://doi.org/10.1007/s12355-020-00919-7>.
- Reinermann, S., Asam, S., Kuenzer, C., 2020. Remote sensing of grassland production and management – A review. *Remote Sens.* 12, 1949. <https://doi.org/10.3390/rs12121949>.
- Reis, A.A., Werner, J.P.S., Silva, B.C., Figueiredo, G.K.D.A., Antunes, J.F.G., Esquerdo, J. C.D.M., Coutinho, A.C., Lamparelli, R.A.C., Rocha, J.V., Magalhães, P.S.G., 2020. Monitoring pasture aboveground biomass and canopy height in an integrated crop–livestock system using textural information from PlanetScope imagery. *Remote Sens.* 12, 2534. <https://doi.org/10.3390/rs12162534>.
- Rosa, D., Basso, B., Fasiolo, M., Friedl, J., Fulkerson, B., Grace, P.R., Rowlings, D.W., 2021. Predicting pasture biomass using a statistical model and machine learning algorithm implemented with remotely sensed imagery. *Comput. Electron. Agric.* 180, 105880. <https://doi.org/10.1016/j.compag.2020.105880>.
- Rouse, J.W., Haas, R.H., Scheel, J.A., Deering, D.W., 1974. Monitoring vegetation systems in the great plains with ERTS. In: *Proceedings, 3rd Earth Resource Technology Satellite (ERTS) Symposium*, vol. 1, pp. 48–62. <https://ntrs.nasa.gov/citations/19740022614>.
- Rouquette Jr., F.M., 2016. Invited Review: The roles of forage management, forage quality, and forage allowance in grazing research. *Prof. Anim. Sci.*, 32, 10–18. <https://doi.org/10.15232/pas.2015-01408>.
- Roy, D.P., Li, J., Zhang, H.K., Yan, L., Huang, H., Li, Z., 2017. Examination of Sentinel-2A multi-spectral instrument (MSI) reflectance anisotropy and the suitability of a general method to normalize MSI reflectance to nadir BRDF adjusted reflectance. *Remote Sens. Environ.* 199, 25–38. <https://doi.org/10.1016/j.rse.2017.06.019>.
- Santos, C.O., Mesquita, V.V., Parente, L.L., Pinto, A.S., Ferreira, L.G., 2022. Assessing the wall-to-wall spatial and qualitative dynamics of the Brazilian pastureslands 2010–2018, based on the analysis of the Landsat data archive. *Remote Sens.* 14, 1024. <https://doi.org/10.3390/rs14041024>.
- Santos, M.L., Santos, P.M., Barioni, L.G., Pereira, B.H., Cuadra, S.V., Pequeno, D.N.L., Marin, F.R., Sollenberger, L., 2024. Yield gap analysis framework applied to pasture-based livestock systems in Central Brazil. *Field Crops Res.*, 314, 109416. <https://doi.org/10.1016/j.fcr.2024.109416>.
- Schaefer, M.T., Lamb, D.W., 2016. A combination of plant NDVI and LiDAR measurements improve the estimation of pasture biomass in tall fescue (*Festuca arundinacea* var. fletcher). *Remote Sens.* 8, 109. <https://doi.org/10.3390/rs8020109>.
- Schmidt, M., Carter, J., Stone, G., O'Reagain, P., 2016. Integration of optical and X-band radar data for pasture biomass estimation in an open savannah woodland. *Remote Sens.* 8, 989. <https://doi.org/10.3390/rs8120989>.
- Schucknecht, A., Meroni, M., Kayitakire, F., Boureima, A., 2017. Phenology-based biomass estimation to support rangeland management in semi-arid environments. *Remote Sens.* 9, 463. <https://doi.org/10.3390/rs9050463>.
- Sekaran, U., Lai, L., Ussiri, D.A.N., Kumar, S., Clay, S., 2021. Role of integrated crop–livestock systems in improving agriculture production and addressing food security – A review. *J. Agric. Food Res.* 5, 100190. <https://doi.org/10.1016/j.jafr.2021.100190>.
- Shahi, T.B., Balasubramanian, T., Sabir, K., Nayak, R., 2025. Pasture monitoring using remote sensing and machine learning: A review of methods and applications. *Remote Sens. Appl. Soc. Environ.*, 37, 101459. <https://doi.org/10.1016/j.rsase.2025.101459>.
- Sibanda, M., Mutanga, O., Rouget, M., 2016. Comparing the spectral settings of the new generation broad and narrow band sensors in estimating biomass of native grasses grown under different management practices. *Gisci. Remote Sens.*, 53, 614–633. <https://doi.org/10.1080/15481603.2016.1221576>.
- Silva, F.S., Domiciano, L.F., Gomes, F.J., Sollenberger, L.E., Pedreira, C.G., Pereira, D.H., Pedreira, B.C., 2020a. Herbage accumulation, nutritive value and beef cattle production on marandu palisadegrass pastures in integrated systems. *Agrofor. Syst.* 94, 1891–1902. <https://doi.org/10.1007/s10457-020-00508-3>.
- Silva, A.D.A., Schmitt Filho, A.L., Kazama, D.D.S., Loss, A., Souza, M., Piccolo, M.D.C., Sinigalli, P.D.A., 2020b. Carbon and nitrogen stocks in the high biodiversity silvopastoral system: applied nucleation enabling low carbon livestock production. *Res. Soc. Dev.* 9, 10. <https://doi.org/10.33448/rsd-v9i10.8589>.
- Silva, Y.F., Valadares, R.V., Dias, H.B., Cuadra, S.V., Campbell, E.E., Lamparelli, R.A.C., Moro, E., Battisti, R., Alves, M.R., Magalhães, P.S.G., Figueiredo, G.K.D.A., 2022. Intense pasture management in Brazil in an integrated crop–livestock system simulated by the DayCent model. *Sustainability* 14, 3517. <https://doi.org/10.3390/su14063517>.
- Slayi, M., Zhou, L., Dzvene, A.R., Mpanyaro, Z., 2024. Drivers and consequences of land degradation on livestock productivity in Sub-Saharan Africa: A systematic literature review. *Land* 13, 1402. <https://doi.org/10.3390/land13091402>.
- Soares, D.A., Lupatini, G.C., Sekiya, B.M.S., Mateus, G.P., Andrighetto, C., Modesto, V.C., Silva, J.R., Luz, J.H.S., Galindo, F.S., Crusciol, C.A.C., Pavinato, P.S., Andreotti, M., 2024. Integrated crop–livestock systems as a strategy for the sustainable production of corn and soybean grain in tropical sandy soils. *Agronomy* 14, 2071. <https://doi.org/10.3390/agronomy14092071>.
- Sousa-Baracho, I.P., Nery, M.C., Rocha, W.W., Farzeni, M.M., Valeriano, F.R., Bento, B. M.C., Rocha, A.S., Carvalho, R.d.C.R., 2024. Assessment for forage grass quality submitted to compaction degrees and nitrogen doses. *Grass Res.* 4, e008.
- Souza, C.M., Shimbo, J.Z., Rosa, M.R., Parente, L.L., Alencar, A.A., Rudorff, B.F.T., Hasenack, H., Matsumoto, M., Ferreira, L.G., Souza-Filho, P.W.M., Oliveira, S.W., Rocha, W.F., Fonseca, A.V., Marques, C.B., Diniz, C.G., Costa, D., Monteiro, D., Rosa, E.R., Vêlez-Martin, E., Weber, E.J., Lenti, F.E.B., Paternost, F.F., Pareyn, F.G. C., Siqueira, J.V., Viera, J.L., Ferreira Neto, L.C., Saraiva, M.M., Sales, M.H., Salgado, M.P.G., Vasconcelos, R., Galano, S., Mesquita, V.V., Azevedo, T., 2020. Reconstructing three decades of land use and land cover changes in Brazilian biomes with Landsat archive and Earth Engine. *Remote Sens.* 12, 2735. <https://doi.org/10.3390/rs12172735>.
- Subhashree, S.N., Igathinathane, C., Akyuz, A., Borhan, M., Hendrickson, J., Archer, D., Liebig, M., Toledo, D., Sedivec, K., Kronberg, S., Halvorson, J., 2023. Tools for predicting forage growth in rangelands and economic analyses—A systematic review. *Agric.* 13, 455. <https://doi.org/10.3390/agriculture13020455>.
- Teixeira, A.H., 2009. Water productivity assessments from field to large scale: A case study in the Brazilian semi-arid region. Lambert Academic Publishing, Saarbrücken, Germany.
- Teixeira, A.H.D.C., 2010. Determining regional actual evapotranspiration of irrigated crops and natural vegetation in the São Francisco river basin (Brazil) using remote sensing and Penman-Monteith equation. *Remote Sens.* 2, 1287–1319. <https://doi.org/10.3390/rs0251287>.
- Teixeira, A.H.C., Hernandez, F.B.T., Lopes, H.L., Scherer-Warren, M., Bassoi, L.H., 2013. A comparative study of techniques for modeling the spatiotemporal distribution of heat and moisture fluxes at different agroecosystems in Brazil, in: *Tropopoulos, G.G. (Ed.), Remote Sensing of Energy Fluxes and Soil Moisture Content*. pp. 165–188. DOI: 10.1201/b15610-9.
- Teixeira, A.H.C., Padovani, C.R., Andrade, R.G., Leivas, J.F., Victoria, D.C., Galdino, S., 2015. Use of MODIS images to quantify the radiation and energy balances in the Brazilian Pantanal. *Remote Sens.* 7, 14597–14619. <https://doi.org/10.3390/rs71114597>.
- Teixeira, A., Pacheco, E., Silva, C., Dompieri, M., Leivas, J., 2021. SAFER applications for water productivity assessments with aerial camera onboard a remotely piloted aircraft (RPA). A rainfed corn study in Northeast Brazil. *Remote Sens. Appl. Soc. Environ.*, 22, 100514. <https://doi.org/10.1016/j.rsase.2021.100514>.
- UNCCD, 2024. Global Land Outlook Thematic Report on Rangelands and Pastoralism. United Nations Convention to Combat Desertification, Bonn. 110 p. Available at: <https://www.unccd.int/sites/default/files/2024-05/GLO%20rangelands%20full.pdf>. Access: 30 jan 2025.
- Varga, K., Csizi, I., Monori, I., Valkó, O., 2021. Threats and challenges related to grazing paddocks: Recovery of extremely overgrazed grassland after grazing exclusion. *Arid Land Res. Manag.* 35, 346–357. <https://doi.org/10.1080/15324982.2020.1869120>.
- Vermote, E., Justice, C., Claverie, M., Franch, B., 2016. Preliminary analysis of the performance of the Landsat 8/OLI land surface reflectance product. *Remote Sens. Environ.* 185, 46–56. <https://doi.org/10.1016/j.rse.2016.04.008>.
- Wang, J., Sun, J., Yu, Z., Li, Y., Tian, D., Wang, B., Li, Y., Niu, S., 2019a. Vegetation type controls root turnover in global grasslands. *Glob. Ecol. Biogeogr.* 28, 1045–1054. <https://doi.org/10.1111/gcb.12866>.
- Wang, J., Xiao, X., Bajgain, R., Starks, P., Steiner, J., Doughty, R.B., Chang, Q., 2019b. Estimating leaf area index and aboveground biomass of grazing pastures using Sentinel-1, Sentinel-2 and Landsat images. *ISPRS J. Photogramm. Remote Sens.* 154, 189–201. <https://doi.org/10.1016/j.isprsjprs.2019.06.007>.
- Vinholis, M.D.M.B., Souza Filho, H.M.D., Shimata, I., Oliveira, P.P.A., Pedroso, A.D.F., 2021. Economic viability of a crop–livestock integration system. *Ciência Rural* 51, e20190538. <https://doi.org/10.1590/0103-8478cr20190538>.
- Wang, L., Jiao, W., MacBean, N., Rulli, M.C., Manzoni, S., Vico, G., D'Odorico, P., 2022. Dryland productivity under a changing climate. *Nat. Clim. Change* 12 (11), 981–994. <https://doi.org/10.1038/s41558-022-01499-y>.
- Wilm, H.G., Costello, D.F., Klipple, G.E., 1944. Estimating forage yield by the double-sampling method. *Agron. J.* 36, 194–203. <https://doi.org/10.2134/agronj1944.00021962003600030003x>.
- Wilson, J.R., Mannelje, L., 1978. Senescence, digestibility and carbohydrate content of buffel grass and green panic leaves in swards. *Aust. J. Agric. Res.* 29, 503–516. <https://doi.org/10.1071/AR9780503>.
- Xie, J., Wang, C., Ma, D., Chen, R., Xie, Q., Xu, B., 2022. Generating spatiotemporally continuous grassland aboveground biomass on the Tibetan Plateau through PROSAIL model inversion on Google Earth Engine. *IEEE Trans. Geosci. Remote Sens.*, 60, 1–14. <https://doi.org/10.1109/TGRS.2022.3227565>.
- Xue, J., Anderson, M.C., Gao, F., Hain, C., Yang, Y., Knipper, K.R., Kustas, W.P., Yang, Y., 2021. Mapping daily evapotranspiration at field scale using the Harmonized Landsat and Sentinel-2 dataset, with sharpened VIIRS as a Sentinel-2 thermal proxy. *Remote Sens.* 13, 3420. <https://doi.org/10.3390/rs13173420>.
- Yan, J., Zhang, G., Ling, H., Han, F., 2022. Comparison of time-integrated NDVI and annual maximum NDVI for assessing grassland dynamics. *Ecol. Indic.*, 136, 108611. <https://doi.org/10.1016/j.ecolind.2022.108611>.

- Yang, S., Feng, Q., Liang, T., Liu, B., Zhang, W., Xie, H., 2018. Modeling grassland above-ground biomass based on artificial neural network and remote sensing in the Three-River Headwaters Region. *Remote Sens. Environ.* 204, 448–455. <https://doi.org/10.1016/j.rse.2017.10.011>.
- Zhang, B., Wu, Y., Zhao, B., Chanussot, J., Hong, D., Yao, J., Gao, L., 2022. Progress and challenges in intelligent remote sensing satellite systems. *IEEE J. Sel. Top. Appl. Earth Obs. Remote Sens.* 15, 1814–1822. <https://doi.org/10.1109/JSTARS.2022.3148139>.
- Zeng, N., Ren, X., He, H., Zhang, L., Zhao, D., Ge, R., Li, P., Niu, Z., 2019. Estimating grassland aboveground biomass on the Tibetan Plateau using a random forest algorithm. *Ecol. Indic.* 102, 479–487. <https://doi.org/10.1016/j.ecolind.2019.02.023>.
- Zhu, Z., Wang, S., Woodcock, C.E., 2015. Improvement and expansion of the Fmask algorithm: Cloud, cloud shadow, and snow detection for Landsats 4-7, 8, and Sentinel 2 images. *Remote Sens. Environ.* 159, 269–277. <https://doi.org/10.1016/j.rse.2014.12.014>.